

Characterization of astrocytes derived from fibroblasts of patients with amyotrophic lateral sclerosis

Mahshad Kolahdouzan

Center for Research in Neuroscience
Research Institute of McGill University Health Center
Integrated Program in Neuroscience
McGill University
April 2019

A thesis submitted to McGill University in partial fulfillment of the requirements of the
degree of Master of Neuroscience - © **Mahshad Kolahdouzan - 2019**

Table of contents

	Page
Abstract -----	ii
Acknowledgements -----	iii
Contribution of Author -----	iv
Chapter 1 – Introduction, objectives and comprehensive literature review -----	1
Chapter 2 – Materials and methods -----	18
Chapter 3 – Evaluating astrocytes derived from three protocol -----	28
Chapter 4 – Characterization of stem-cell derived ALS astrocytes -----	41
Chapter 5 – Discussion, conclusions, limitations and future directions -----	44
References -----	55

Abstract

Amyotrophic lateral sclerosis (ALS) is a fatal neuromuscular degenerative disease, targeting the motor neurons of the brain stem, motor cortex and spinal cord. Various lines of evidence have shown that glial cells contribute to disease development and progression. We derived astrocytes from fibroblasts of patients with familial ALS associated with SOD1 mutation and compared them to astrocytes derived from fibroblasts of age- and sex-matched controls. In order to assess astrocytic maturity, we compared the mRNA expression of astrocytic markers in astrocytes derived from three different protocols to that of human fetal astrocytes (HFA). Protocol 1 incorporated 10 weeks of astrogenesis. Protocol 2 incorporated 3 weeks of neurogenesis and 10 weeks of astrogenesis, and protocol 3 incorporated 2 weeks of astrogenesis. Our data show that astrocytes from all three protocols are similar in mRNA expression of astrocytic markers to HFA. However, morphologically, astrocytes from protocol 1 and 2 had astrocyte-like projections and therefore looked more like astrocytes compared to astrocytes from protocol 3. Next, we derived astrocytes from ALS patients, using protocol 2 and compared them to their age- and sex-matched controls. We found that the mRNA levels of EAAT2 and NESTIN were lower and the mRNA levels of glutamine synthetase, connexin43 and TGFB1 were higher in ALS astrocytes compared to their controls. Since the phenotypes observed in this study corroborate with previous literature exploring the role of astrocytes in ALS, these astrocytes may offer a system in which ALS can be studied in human cells.

Résumé

La sclérose latérale amyotrophique (SLA) est une maladie neuromusculaire et neurodégénérative qui a pour cible les neurones moteurs du tronc cérébral, du cortex moteur et de la moelle épinière. Diverses sources de données ont démontré que les cellules gliales contribuent au développement et à la progression de la maladie. Notre but était de dériver des astrocytes matures à partir de fibroblastes de patients atteints de la SLA et de les comparer à des astrocytes dérivés de fibroblastes provenant de témoins appariés selon l'âge et le sexe. Afin de nous assurer de la maturité astrocytaire, nous avons comparé les niveaux d'expression de l'ARNm de marqueurs astrocytaires dans des astrocytes obtenus par 3 protocoles différents aux niveaux de ces marqueurs dans des astrocytes fœtaux humains (AFH). Le protocole 1 incorporait 10 semaines d'astrogénèse. Le protocole 2 incorporait 3 semaines de neurogénèse suivies de 10 semaines d'astrogénèse, et le protocole 3 incorporait 2 semaines d'astrogénèse. Nos données montrent que les astrocytes issus de chacun des trois protocoles ont des niveaux d'expression d'ARNm de marqueurs d'astrocytes similaires aux niveaux d'expression dans les AFH. Cependant, morphologiquement, les astrocytes des protocoles 1 et 2 ressemblaient plus à des astrocytes. Par la suite, nous avons dérivé des astrocytes issus de patients atteints de la SLA en utilisant le protocole 2. Nous les avons comparés à leurs témoins appariés selon l'âge et le sexe. Nous avons découvert que les niveaux d'ARNm de EAAT2 et de NESTIN étaient plus bas et que les niveaux d'ARNm de glutamine synthétase, connexine 43 et TGFB1 étaient plus élevés dans les astrocytes de la SLA comparés aux témoins. Étant donné que les phénotypes observés dans cette étude sont en accord avec la littérature, ces astrocytes pourraient constituer un système dans lequel la SLA serait étudiée dans des cellules humaines.

Acknowledgements

I would like to thank Dr. David Stellwagen, for his mentorship and guidance through my graduate studies. I would also like to thank my advisory committee, Drs. Carl Ernst and Edward Ruthazer, for their continued support and encouragement and for also sharing with me their expertise and helping guide my project along.

I also thank Marie Franquin, without whom this project would be impossible for me to complete. Thank you for teaching me most of the skills I needed to know, from working with stem cells, to deriving neuron progenitor cells, and performing an immunocytochemistry, and thank you for your guidance and support throughout. And of course, thank you for being a loving friend throughout it all.

I want to thank Renu Heir, who taught me how to complete a qPCR experiment and has taught me so much about biochemistry, tissue and cell culture, and science and life in general. My graduate studies would not have been as smooth without you. I also want to extend a thank you to the rest of the Stellwagen team, who were great colleagues and friends. I also thank Blandine Ponroy, who taught me how to develop astrocytes from neuron progenitor cells. Thank you to Drs. Jack Antel and and Luke Healy for providing us with human fetal astrocytes.

I want to thank my support system outside of the lab, to Elnaz, Dorothy, Maansi, Danny and Mazen, I couldn't have done this without your unconditional love and support.

Of course, thank you to Dr. Ibrahim Kays, who has inspired me in more ways than I thought possible. You helped me rediscover my passion for science. And last but not least, to my parents, Maryam and Majid, and my brother Kouros, to whom I owe everything. Thank you for your

unconditional love and support through all the uncertainty and hardships that this career path brings.

Contribution of Author

Derivation of NPCs from stem cells was done by both Mahshad Kollahdouzan and Marie Franquin. Culturing the NPCs and driving towards astrocytic fate using the three different protocols was done by Mahshad Kollahdouzan. Protocol 1 was adapted from Blandine Ponroy from Dr. Keith Maurai's lab. The data collected using qPCR and immunocytochemistry was conducted by Mahshad Kollahdouzan. Dr. Luke Healy from Dr. Jack Antel's lab gifted us with human fetal astrocytes. All chapters were written by Mahshad Kollahdouzan.

Chapter 1 – Introduction, objectives and comprehensive literature review

Introduction

Jean-Martin Charcot first used the term “amyotrophic lateral sclerosis” in 1874 to describe a disease associated with progressive muscle atrophy, as well as protopathic spinal amyotrophy, resulting in motor weakness (Goetz, 2000). Amyotrophic lateral sclerosis (ALS) is a fatal neuromuscular degenerative disease that preferentially targets motor neurons of the motor cortex, brainstem and spinal cord, causing progressive muscle paralysis, leading to death 3-5 years post symptom onset on average (Dadon-Nachum, Melamed, & Offen, 2011). Also known as Lou Gehrig’s disease in the United States, and motor neuron disease in the United Kingdom (Taylor, Brown Jr, & Cleveland, 2016), ALS is the most common form of motor neuron disease, usually affecting adults between the ages of 45 and 60 years, with an incidence of 1-2 per 100,000 individuals per year (Dadon-Nachum et al., 2011).

Depending on the location of primary pathology, there is significant heterogeneity in the clinical symptoms that patients experience. Progressive muscular atrophy, affecting the spinal cord or the lower motor neurons results in weakness in the limbs as the first symptoms of the disease.

However, primary lateral sclerosis, mainly affecting corticospinal motor neurons results in hyperflexia and spasticity. Bulbar ALS, affecting brainstem motor neurons results in tongue atrophy, thickness of speech and difficulty swallowing. As well, ALS shows clinical overlaps with other adult-onset degenerative disorders, such as frontotemporal dementia (FTD) (Taylor et al., 2016).

Until recently, Riluzole, which has anti-glutamnergic effects through the inhibition of glutamate release, was the only form of approved treatment for ALS patients and only extends the patient survival by 2 to 3 months (Geevasinga et al., 2016). However, in 2018, another FDA-approved drug became available to ALS patients, called edaravone, which is a free radical scavenger and

targets peroxynitrite, and has shown to result in slower progression and better prognosis in ALS patients (Okada et al., 2018). Several mechanisms contribute to the pathogenesis of ALS, including oxidative stress, protein aggregation, mitochondrial dysfunction, neuroinflammation, impaired cell stress response and apoptosis, making this a complex and multi-faceted disease (Pasinelli & Brown, 2006).

About 90% of ALS cases are sporadic (sALS), presenting without a family history of the disease, while the remaining 10% of the cases are familial (fALS), inherited from family members as dominant traits (Taylor et al., 2016). The first ALS gene, cytosolic superoxide dismutase (SOD1) was reported in 1993 (Rosen et al., 1993), and about 20% of fALS and 5% of the sALS cases are associated with a mutation in SOD1, resulting in toxic gain or loss of the protein function (Bunton-stasyshyn, Saccon, Fratta, & Fisher, 2015; Saccon, Bunton-stasyshyn, Fisher, & Fratta, 2013). The most common genetic mutation in ALS is C9orf72, with 25% of fALS cases and 10% of sALS cases associated with this mutation (Taylor et al., 2016). fALS and sALS have similar pathophysiology, and studying familial genetic mutations, such as SOD1 mutations, could uncover mechanisms common to both types of the disease (Bunton-stasyshyn et al., 2015; Saccon et al., 2013).

Glial contribution to ALS

Although the exact pathology in ALS remains unknown, glial activation has been shown to begin before or at disease onset in animal models of the disease (Alexianu, Kozovska, & Appel, 2001; Kriz, Nguyen, & Julien, 2002; Vargas & Johnson, 2010), and glia contribute to development and progression of the disease (Lasiene & Yamanaka, 2011). As well, expression of human SOD1 protein with G37R mutation only in motor neurons of mice did not result in disease development or progression (Pramatarova, Laganière, Roussel, Brisebois, & Rouleau, 2001), therefore

suggesting the involvement of glia in ALS pathogenesis. Further, chimeric mice carrying SOD1G37R mutation in neurons or oligodendrocytes did not develop motor neuron loss (K. Yamanaka et al., 2008). However, expression of mutant SOD1 in microglia or astrocytes have shown to be toxic to motor neurons and contribute to disease progression (Boillée, Yamanaka, et al., 2006; Clement et al., 2003; Marchetto et al., 2008; Rojas, Cortes, Abarzua, Dyrda, & van Zundert, 2014). Therefore, these findings suggest that neuronal expression of mutant SOD1 is not enough to result in the development of ALS, warranting the investigation of glial contribution, such as microglia or astrocytes, to the disease.

Astrocytes

Since their discovery, astrocytes have emerged as the most abundant cell type in the brain, with a variety of functions. Astrocytes are commonly found in close proximity to pre- and post-synaptic neurons at the excitatory synapse, forming an arrangement called “tripartite synapse”. One of the functions of astrocytes is homeostatic maintenance of neurotransmitters, such as glutamate and GABA. Astrocytes have high affinity transporters for these neurotransmitters and provide glutamine, the precursor for glutamate and GABA (Schousboe, Bak, & Waagepetersen, 2013). In addition to being close to the synapse, astrocytes also contact and surround blood vessels in the brain, regulating blood flow and contributing to the maintenance of blood brain barrier (Gorshkov, Aguisanda, Thorne, & Zheng, 2018). Astrocytes also maintain extracellular ion homeostasis through regulation and uptake of molecules such as K^+ and water, via Na^+/K^+ pump, Kir4.1 and Aquaporin 4 (AQP4) (Kimelberg & Nedergaard, 2010). Inward rectifying K^+ channel Kir4.1 are primarily responsible for regulation of baseline K^+ levels in the extracellular space, whereas the Na^+/K^+ pump determines the rate of extracellular K^+ level recovery after excessive neuronal firing in hippocampal slices. Further, astrocytes constitute the major route for water

transport in and out of the brain via expression of AQP4 in the vascular end-feet astrocytes (Kimelberg & Nedergaard, 2010). Another important function of astrocytes is guiding the formation and maturation of synapses. For example, *Christopherson et al.* found that thrombospondin-1 and -2, released by astrocytes, were necessary and sufficient to stimulate excitatory synapse formation (Christopherson et al., 2005). Discovering these astrocytic functions has led to a shift in focus with regard to the roles of astrocytes in neurodegenerative diseases, leading to astrocyte-specific analyses, with potential for drug discoveries and therapeutic development. For instance, in Alzheimer's disease, Huntington's disease and ALS, astrocytes change their activation state, shape and molecular expression patterns, and may contribute to disease (Maragakis & Rothstein, 2006; Koji Yamanaka & Komine, 2017).

Astrocytes and ALS

Various lines of evidence have shown that in ALS, astrocytes change in expression profile of astrocytic and inflammatory markers, morphology and activation state, becoming toxic to motor neurons, both *in vivo* and *in vitro*, hence affecting disease development and progression.

In the lumbar spinal cord from SOD1G93A rats, astrocytes progressively acquire a reactive morphology, with an increase in GFAP and S100B expression (Serrano et al., 2017). 72 hours after transfection with A4V SOD1-EGFP, the cell-viability of astrocytes is reduced by 50% *in vitro*, compared to wildtype control (Wallis et al., 2017). Astrocytes transfected with A4V SOD1-EGFP had lower glutamate transporter (EAAT) activity and had a more reactive phenotype as shown by their stellate morphology and GFAP expression, after 72 hours. Further, non-transfected astrocytes adjacent to A4V SOD1-EGFP astrocytes had significantly a more reactive phenotype compared to non-transfected astrocytes adjacent to WT SOD1-EGFP astrocytes (Wallis et al., 2017). *In vivo*, reduction of SOD1G37R in astrocytes extended survival

of mutated mice by 48 days (Koji Yamanaka et al., 2008)., SOD1G93A astrocytes transplanted into the spinal cord of wild-type rats resulted in motor neuron death and decline in hindlimb grip strength (Papadeas, Kraig, O'Banion, Lepore, & Maragakis, 2011). The disease-inducing property of ALS astrocytes was also shown in another study, where astrocytes from sALS patients with a C9Orf72 mutation transplanted into the spinal cord of wildtype mice induced toxicity to motor neurons, which corresponded to mouse motor behavioural deficits (Qian et al., 2017).

Astrocytic toxicity to motor neurons

Motor neurons co-cultured with astrocytes derived from fALS and sALS patient neuron progenitor cells (NPCs), obtained from post mortem tissue, began to degenerate after 96 hours (Haidet-phillips et al., 2012). human motor neurons co-cultured with astrocytes from G93A mice for 30 days had prominent phosphorylated neurofilament heavy chain (pNF-H) aggregates, which is linked to disease progression and is considered an ALS biomarker (Tripathi et al., 2017). Indeed, motor neurons treated with fALS and sALS astrocyte conditioned media also died 50% faster than motor neurons conditioned with media from non-ALS astrocytes. Further, primary fetal astrocytes transfected with SOD1G37R were toxic to motor neurons derived from human embryonic stem cells, resulting in 49% reduction in survival compared to motor neurons cocultured with control astrocytes (Marchetto et al., 2008). Taken together, these data suggest that it is not only through contact that astrocytes may be toxic to neurons, but rather that astrocytes may also release toxic factors that result in oxidative stress and motor neuron death.

.Astrocytes transfected with mutant SOD1 activated an inflammatory response, an effect that was counteracted with antioxidants, resulting in the rescue of the motor neurons (Marchetto et al., 2008). As well, adding antioxidant Trolox (water-soluble vitamin E analog that neutralizes ROS)

and esculetin to SOD1G85R astrocyte-conditioned media rescued motor neuron death (Rojas et al., 2014). Another factor that may contribute to astrocytic toxicity towards motor neurons is the pro-inflammatory cytokine TGF β 1, which was found to be released at high levels in SOD1 mutant mouse astrocyte cultures (Tripathi et al., 2017). Further, astrocytes from G93A mice were toxic to healthy human motor neurons *in vitro*. Treating human motor neurons with TGF β 1 alone resulted in an ALS-like phenotype, with pNF-H aggregates, an effect that was rescued when TGF β 1 levels were reduced (Tripathi et al., 2017). Another factor that may contribute to neuroinflammation is S100B. In spinal cord of wildtype mice, S100B is expressed at low levels, mostly in the white matter (Serrano et al., 2017). However, S100B is higher in SOD1G93A tissue, particularly in GFAP-positive astrocytes with typical reactive phenotypes. The levels of pro-inflammatory cytokines, such as TNF were higher in astrocytes of SOD1G93A mice, and when S100B levels were reduced in astrocytes of SOD1G93A mice, the levels of pro-inflammatory cytokines reduced as well. The reason S100B may be pro-inflammatory at high levels is that S100B may act as an endogenous alarm signal, known as danger-associated molecular pattern (DAMP), and may activate RAGE, a receptor associated with neuroinflammation. Indeed, in SOD1G93A mice, the levels of RAGE are high at endstage of the disease and co-localize with S100B expression (Serrano et al., 2017). Previous studies have found that oxidative stress and neuroinflammation can activate apoptosis, resulting in neuronal death (Reviewed in: Kollahdouzan and Hamadeh, 2017). Indeed, when astrocytes from G93A mice were co-cultured with wild-type neurons, the levels of fractin, which is a fragment of B-actin generated by activated caspase-3, was higher *in vitro* (Nagai et al., 2007). However, this phenotype was rescued when Bax, a proapoptotic protein, was inhibited. Therefore, ALS astrocytes may activate apoptosis in motor neurons, through the induction of neuroinflammation.

Another potential mechanism regarding astrocytic toxicity in ALS is the disruption of blood brain barrier integrity. In healthy conditions, AQP4 is mostly expressed at the astrocyte endfeet surrounding blood vessels (Watanabe-Matsumoto et al., 2017). However, in SOD1G93A mouse astrocytes, AQP4 was mislocalized during the progression of ALS symptoms. As well, the protein levels of AQP4 were higher in ALS mice. In human post-mortem tissue, AQP4 was also higher in one patient with fALS-SOD1 mutation and seven out of eight patients with sALS. Further, when AQP4 was knocked out in G93A mice, blood brain barrier disruption was improved. However, AQP4 knockout also resulted in early disease onset and shorter lifespan in G93A mice (Watanabe-Matsumoto et al., 2017). Another protein expressed on astrocytes is Kir4.1, which is an inward rectifying potassium channel that helps maintain the CNS extracellular ion balance and the blood brain barrier integrity (Bataveljic, Nikolic, Milosevic, Todorovic, & Andjus, 2012). Kir4.1 levels were lower in the brainstem and spinal cord of SOD1G93A rats (Bataveljic et al., 2012; Kelley et al., 2018)

In primary glial cultures from spinal cord of SOD1G93A rats at the post-symptomatic stage (175d), ALS astrocytes were more proliferative than their wildtype counterparts, had lower levels of EAAT2 and higher S100B and Cx43 levels, and induced motor neuron death (Díaz-amarilla et al., 2011). Glutamate excitotoxicity, due to higher concentration of glutamate in the synapse, has been proposed as a potential mechanism underlying ALS pathophysiology. Higher concentration of glutamate can be due to increased release of glutamate from the presynaptic neuron, or lower rate of reuptake by the neuron or the astrocyte in the synapse (Lin, King, Cuny, & Glicksman, 2013). EAAT1 and EAAT2 together are responsible for glutamate transport into astrocytes, with EAAT2 being responsible for 80-90% of the overall glutamate transport, and their role is glutamate uptake from the synapse into the astrocyte, where glutamate is converted

to glutamine via glutamine synthetase (GS) and recycled back to the neuron (Lin et al., 2013; Suárez, Bodega, & Fernández, 2002). Studies from human post mortem tissue, as well as animal models, have shown that both fALS and sALS astrocytes have lower EAAT2 levels, therefore potentially taking up less glutamate and contributing negatively to disease progression (Chandrasekaran, Avci, Leist, Kobolák, & Dinnyés, 2016). Further, ALS astrocytes also have higher levels of GS, and when GS was inhibited in these astrocytes, the levels of glutamate in the synapse also decreased (Bos et al., 2006; Ghoddoussi et al., 2010). Therefore, changes in astrocytic expression profile and function may contribute to disease development and progression in a non-cell autonomous manner, in ALS. However, most of these findings are from animal models and findings from animal models have not translated to human patients of ALS. This has highlighted the need for a human model system to complement the animal models of the disease. One of the proposed human models are human induced pluripotent stem cells, which can be derived from virtually any cell type.

Patient-derived cells – studies on human cells

Most of the findings regarding disease pathology and underlying mechanisms are based on studies done on rodents. However, human and rodent astrocytes differ in genetic expression, morphology and function (Zhang et al., 2016). Therefore, animal models may not recapitulate the human disease very well. Indeed, success in clinical trials has been extremely limited, questioning the translation efficacy of the preclinical data, from animals, into humans (Benatar, 2007). Therefore, there is a need to find models that closely resemble the human physiology, in order to model human diseases better.

Human induced pluripotent stem cells (hiPSCs) are a model to study human diseases in human cells, via reprogramming any cell type into pluripotent stem cells, through inducing the

expression of four pluripotency genes, (Takahashi & Yamanaka, 2006) as shown in Figure 1.. Since their development, hiPSCs have been proposed as models to study neurodegenerative disorders, such as ALS. Most of these studies focus on differentiating the hiPSCs into motor neurons, while some differentiate the stem cells into astrocytes (Chandrasekaran et al., 2016; Thonhoff, Ojeda, & Wu, 2009). Therefore, stem-cell derived neurons and glia have been proposed as a model to study ALS, in an effort to complement the observations in animal models and understand the human disease better.

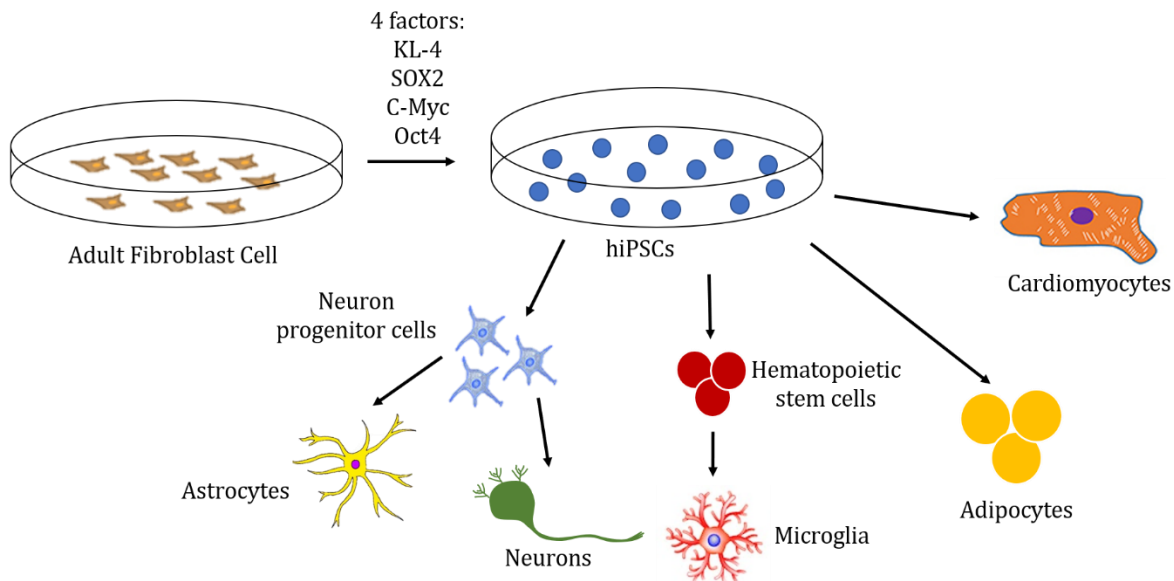


Figure 1. Human induced pluripotent stem cell (hiPSC) development and differentiation.

Fibroblasts, obtained from healthy subjects or patients, are transfected with four factors (KL-4, SOX2, C-Myc, and Oct4). The transfected cells then turn to stem cells and form stem cell colonies. The stem cell colonies can be derived virtually into any cell type, such as cardiomyocytes, adipocytes, microglia, neurons and astrocytes (Figure adapted from Amabile, G. & A. Meissner (2009) Trends Mol. Med. 15:59.).

When astrocyte-like cells, directly converted from fibroblasts of patients with SOD1A4V and C9Orf72 mutations, were co-cultured with motor neurons, the survival rate of the motor neurons was reduced by 60-80%, compared to motor neurons co-cultured with control astrocytes (Meyer et al., 2014). iPSC-derived astrocytes with TDP-43M337V mutation had more cytoplasmic TDP-43 and reduced survival rate, compared to control astrocytes (Serio et al., 2013). Conditioned media from patient astrocytes, with C9Orf72 mutations, derived from motor-neuron progenitor cells resulted in lower cell viability of the iPSC-derived motor neurons (Madill et al., 2017).

Protocols for astrocytes derived from stem cells

Several groups have developed protocols for astrocyte development either from NPCs or through direct conversion of fibroblasts (Krencik & Zhang, 2011; Meyer et al., 2014; Paşca, Sloan, Clarke, Tian, & Christopher, 2015; Roybon et al., 2013; Santos et al., 2017; Serio et al., 2013; Shaltouki, Peng, Liu, Rao, & Zeng, 2013; Sloan et al., 2017; TCW et al., 2017). Most of the protocols published to date are summarized in Table 1. For most of the protocols, the markers used to identify astrocytes are GFAP and S100B (Krencik & Zhang, 2011; Meyer et al., 2014; Paşca et al., 2015; Santos et al., 2017; Serio et al., 2013; Shaltouki et al., 2013; TCW et al., 2017). Until recently, expression of GFAP was taken to be sufficient to identify astrocytes. However, GFAP is also expressed in immature astrocytes and NPCs, and its expression varies from one type of astrocyte to the next, and from one part of the CNS to the next (Molofsky & Deneen, 2015). In fact, some astrocytes, such as those of the cortical region, have very low levels of GFAP. Therefore, expression of GFAP or lack thereof does not accurately define astrocytic identity. Beyond marker expression, as shown in Table 1, some studies also demonstrate the functional capacity of astrocytes through glutamate uptake efficiency measurements, astrocytes' ability to induce synaptogenesis, transient calcium waves in response to ATP, spontaneous

calcium waves, and astrocytes' reactivity to inflammatory cytokines. Therefore, along with marker expression, the demonstration of functional capacity of the cells is required to demonstrate astrocytic properties of the derived cells.

Although marker expression, along with functional capacity, has been used to identify astrocytes, it has proven much more difficult to show maturity of astrocytes. In fact, astrocytes derived from most protocols are likely immature, due to their expression of NPC markers such as NESTIN. However, due to the late onset of ALS, there may be important disease-relevant differences between mature and immature astrocytes.

Astrocytic maturation

At the end stages of neurogenesis, radial glia cells in the ventricular zone undergo division, in which one daughter cell inherits the pial fiber and translocates over relatively long distances from the ventricular surface toward the cortical plate (Noctor, Martínez-cerdeño, Ivic, & Kriegstein, 2004). These translocating cells express nestin, vimentin and GFAP, all of which are expressed in immature astrocytes. After neurogenesis is complete, radial glia from the ventricular zone start to move to the cortical plate and transform into astrocytes. Once the neurons develop, they help stimulate and support astrogenesis, by releasing growth factors such as cardiotrophin-1 (Barnabé-Heider et al., 2005). In humans, astrogenesis begins shortly before 17-20 gestation weeks, and the vast majority of mature astrocyte markers, such as ALDH1L1, EAAT1, EAAT2, Cx43 and S100B, rapidly increase in expression soon after birth, peaking at about 6 month to 1 year of age (Zhang et al., 2016). Beyond mature marker expression, ramifications and processes increase in numbers and become more dense and complex as astrocytes mature (Freeman, 2010). Compared to gestation week 17-24, there is a dramatic increase in levels of EAAT2 in postnatal human brain at 6, 12, and 48 months (Bar-peled et al., 1997). As well, the levels of EAAT1 were

lower in the white matter of the human cortex compared to EAAT2, in postnatal tissue. Another specific astrocytic marker is connexin 43 (Cx43), which is a gap junction protein. The protein levels of Cx43 remained high from embryonic day E12 to 6 weeks postnatal in the brain of rats (Dermietzel et al., 1989). However, another study showed that at E12, Cx43 protein levels were low and increased continually until postnatal day 28 in the visual cortex of rats (Nadarajah, Jones, Evans, & Parnavelas, 1997). The difference in findings between these two studies may be due to the fact that Cx43 expression in the visual cortex may be different than that of other regions; therefore, investigating whole-brain Cx43 expression may mask the differential expression of this protein in different regions. ALDH1L1 is another astrocytic marker, that has been shown to be expressed in mice at E9.5, in cells that have distinctive morphology of radial glia and was co-expressed with nestin, a transcription factor expressed in radial glia (Anthony & Heintz, 2007). Further, ALDH1L1 upregulation correlated with decreased proliferation. Therefore, ALDH1L1 may be an early mature astrocytic marker. Another marker associated with astrocytic maturity is S100B, a calcium binding protein expressed in astrocytes and oligodendrocytes (Raponi et al., 2007). In mice, at postnatal day 2, S100B is absent from radial glial cells, which begin to express GFAP. At postnatal day 8, about 10-30% of GFAP+ cells are also S100B+ and harbor a more ramified morphology. By postnatal P14, nestin staining completely disappeared, about 67% of the cells expressed S100B, and the astrocytic morphological maturation was almost complete. Therefore, S100B expression characterized a mature developmental stage in astrocytes, in mice (Raponi et al., 2007).

Therefore, markers such as ALDH1L1, EAAT1, EAAT2, Cx43 and S100B have been identified as mature astrocytic markers (Molofsky & Deneen, 2015). A mix of these markers were used to

identify stem-cell derived mature astrocytes in more recent studies (Meyer et al., 2014; Roybon et al., 2013; Santos et al., 2017; Sloan et al., 2017; TCW et al., 2017).

Indeed, one of the challenges of the field is the lack of knowledge about the characteristics and markers of mature astrocytes compared to those of immature astrocytes. Therefore, validating astrocytes derived from NPCs based on mature astrocyte markers, as well as functional capacity, is may be crucial for using these astrocytes to model diseases.

Rationale

Although ALS was traditionally thought to be a cell-autonomous motor neuron disease, recent studies have found that astrocytes also influence disease progression and motor neuron death (Boillée et al., 2006; Di Giorgio et al., 2007; Haidet-phillips et al., 2012). These findings correlate with observations in animal models where the expression of mutant SOD1 in neurons alone is not enough to result in ALS (Pramatarova et al., 2001). In addition, lower levels of glutamate transporter EAAT2 shown in astrocytes from ALS patients and animal models may result in more glutamate remaining in the synapse, therefore potentially contributing to glutamate excitotoxicity in ALS (Shaw & Eggett, 2000). Human and rodent glia are different in size, morphology and gene expression and may carry out different functions, warranting further study in human cells (Zhang et al., 2016). Therefore, we propose to study glial specific gene and protein expression changes in astrocytes derived from ALS-patient cell lines, in an effort to better understand their contribution to disease development and progression.

Objectives

1. We characterized astrocytes derived from different protocols to find a protocol that results in the most mature astrocytes. We assessed NPC and astrocytic marker mRNA and protein levels in the astrocytes derived from different protocols.
2. We characterized astrocytes derived from fibroblasts of ALS patients compared to their age- and sex- matched controls. We assessed the mRNA levels of astrocytic markers and inflammatory cytokines previously shown to be affected in ALS.

Table 1. Summary of most published protocols for stem-cell derived astrocytes.

Authors	Stage 1	Stage 2	Stage 3	Marker expression	Functional assays
Krencik and Zhang, 2011	Neuroepithelial cells 11 days Media: DMEM/F-12, NEE, N2, heparin Optional: add RA -> caudalize progenitors Add SHH → ventralize progenitors	Progenitors 69 days Media: DMEM/F-12, NEE, N2, heparin, EGF, FGF2	Astrocyte differentiation and maturation 6 days Media: DMEM/F-12, NEE, N2, heparin, CNTF	Protein levels of: - GFAP - S100B - CD44	N/A
Shaltouki et al., 2013	Neural stem cells	Astrocyte differentiation: 1. DMEM/F-1, heregulin, IGFI, activin, FGF2 2. Neurobasal, CNTF, BMP2 3. Neurobasal, CNTF, BMP2, 1% FBS	N/A	Protein levels of: - GFAP - S100B - NFIA - CD44 (intermediate stage before maturation) - NESTIN (low or absent) - SOX1/SOX2 (low or absent)	- Enhance synapse formation - Efficient glutamate uptake - Can integrate <i>in vivo</i>
Serio et al., 2013	Astroglial precursors - EGF and LIF → neurospheres - 4-6 weeks	Astroglial precursor expansion - EGF and FGF2	Astroglial maturation - CNTF - 14 days	- GFAP - S100B	- Can stimulate synaptogenesis - ATP-evoked calcium release
Roybon et al., 2014	NPC - SB431542 and LDN193189 - 5 days	Motor neuron development - RA, SHH, N2, B27 - 35 days	Astrogenesis - B27, FBS	- EAAT2 - BDNF - GDNF	- calcium waves upon stimulation - neurite outgrowth - become reactive in response to inflammatory cytokines
Meyer et al., 2014	Fibroblast conversion to neuron progenitor cells - Transfected with Klf4, Oct-3/4, Sox2, c-Myc	NPC development - EGF + FGF2 + heparin	Astrogenesis - DMEM/F-12, N2, FBS	- Vimentin - CD44 - S100B - GFAP - AQP4	- ALS phenotype - ALS astrocytes were toxic to motor neurons

Pa ca et al., 2015	Human cortical spheroids <ul style="list-style-type: none"> - Knockout serum without FGF2 - Inhibited BMP and TGFB1 with small molecules - After 5 days, NB + B27, FGF2 and EGF - 25 days 	Neuronal differentiation <ul style="list-style-type: none"> - NB, BDNF, NT3 – 18 days - NB and B27 for the remaining time 	Astrogenesis <ul style="list-style-type: none"> - Maintained GFAP+ cells in serum-free culture 	- GFAP	- adopted a reactive phenotype when exposed to serum
TCW et al., 2017	Neuron progenitor cells	Astrocyte differentiation: <ul style="list-style-type: none"> - Commercial astrocyte media – ScienCell - 30 day - 42 cell lines 	N/A	<ul style="list-style-type: none"> - GFAP - S100B - ALDH1L1 - Vimentin - AQP4 - EAAT1 - Similar to primary fetal astrocytes 	<ul style="list-style-type: none"> - -Promote extracellular cell adhesion and interaction - -Secrete cytokines in response to inflammatory stimuli - -Capable of phagocytosis - -Spontaneous calcium transient activity
Santos et al., 2017	Glial precursor development <ul style="list-style-type: none"> - EBs in ScienCell media + noggin - 2 weeks - PDGF – 3 weeks 	Astrocyte differentiation <ul style="list-style-type: none"> - LIF - 4-6 weeks 	N/A	<ul style="list-style-type: none"> - GFAP - S100B - ALDH1L1 - EAAT1 - EAAT2 	<ul style="list-style-type: none"> - Capable of glutamate uptake - Slow calcium transients - Respond to pro-inflammatory stimuli
Sloan et al., 2017	Human cortical spheroids	Isolating astrocytes <ul style="list-style-type: none"> - Immunopanning with HepaCAM 	N/A	<ul style="list-style-type: none"> - AQP4 - SOX9 - EAAT1 	<ul style="list-style-type: none"> - Glutamate uptake capacity - Can phagocytose synaptosomes

Chapter 2 – Materials and methods

Materials and methods

NPC development from hiPSCs

Fibroblasts of 3 healthy individuals (2 male and 1 female, relevant subject information shown in Table 2) were obtained from the Corriell institute, transfected with the 4 Yamanaka factors (KLF4, SOX2, C-Myc and Oct4) and driven towards hiPSCs using a previously established protocol (described here (Bell et al., 2016)). hiPSCs were plated in 6 well plates, coated with Matrigel, in conventional stem-cell maintaining media containing mTsr1 and rock inhibitor Y-27632. When hiPSCs reached a density of 20-30%, differentiation towards NPCs began. Cells were placed in neural induction media 1 (NIM1 – DMEM/F12, N2, B27, BSA, NEAA, SB431542, noggin and laminin) for 7 days, and media was changed every two days. On the 8th day of induction, cells were placed in neural induction media 2 (NIM2 - DMEM/F12, N2, B27, BSA, NEAA, and laminin) for 7 days and media was changed every day. On day 14th of induction, the cells were dissociated, using Gentle Cell Dissociation reagent and replated on Matrigel-coated tissue culture dishes. At this stage, cells were classified as NPCs, as determined by the expression of NPC markers NESTIN, SOX1 and SOX2, and once they reached 90% confluency, we split the cells, froze 60% of the cells, and used the remaining 40% of the cells for astrocytic differentiation, as described below.

	Age	Sex
Subject #1	57	Male
Subject #2	61	Male
Subject #3	51	Female

Table 2. Characteristics of healthy subjects. Fibroblasts of 3 healthy subjects were obtained. Subjects were 57 (male), 61 (male) and 51 (female) years old.

Human fetal astrocytes

Human fetal astrocytes (HFA) were obtained from the Antel lab. The cells were isolated from human fetal brain at 20th week of gestation, as previously described (Jack et al., 2005). In short, HFA were obtained by dissociation of the fetal CNS with trypsin and DNase I, followed by mechanical dissociation. The cells were plated on Matrigel coated dishes, and their media (DMEM/F12 and 10% FBS) was changed every 2-3 days. Cells were extracted when confluent.

Astrocyte differentiation and maturation

We assessed three different protocols (shown in Figure 2) for astrocytic development, using one biological replicate of 3 different cell lines from 3 healthy subjects.

Protocol 1 was adapted from our collaborators (Dr. Keith Murai and Blandine Ponroy), and, by incorporating growth factors CNTF, FGF-2 and EGF, it closely emulated what other groups have also incorporated into their astrocyte differentiation protocols (Krencik & Zhang, 2011; Serio et al., 2013; Shaltouki et al., 2013). Briefly, NPCs, generated from hiPSCs, underwent three stages of astrogenesis. NPCs were plated on Matrigel, and when they reached 60-70% confluence, they were placed in astrocyte differentiation media 1 (ADM1 – DMEM/F12, 10% FBS, 20ug/ml FGF2, and 20 ug/ml of EGF) for two weeks. Media was changed every 2-3 days. On the first day of the 3rd week of astrocyte differentiation, astrocytes were placed in ADM 2 (DMEM/F12, 10% FBS, 20ug/ml FGF2, and 20 ug/ml of EGF and 5 ug/ml of CNTF), and the astrocytes were in ADM 2 for 6 weeks. On the first day of the 9th week of astrocytic differentiation, astrocytes were placed in ADM 3 (DMEM/F12, 10% FBS, and 5 ug/ml of CNTF) for two weeks. The media on the cells was changed every 2-3 days, and the cells were split 3/10 and replated every time they reached confluency. The frequency of reaching confluency was different between different cell

lines, as some cell lines grew faster than others. However, on average, in the first 6 weeks, the cells reached confluency once a week and were split once a week, and towards the end of the protocol, growth rate decreased and we split the cells about once every 2-3 weeks, if at all.

In order to achieve astrocytic maturity, we created a protocol that more closely emulated astrogenesis *in vivo*. During development, astrogenesis occurs after neurogenesis, and once the neurons develop they support and stimulate astrogenesis by releasing factors such as cardiotrophin-1 (Barnabé-Heider et al., 2005). In order to achieve spinal astrocyte maturity, Roybon *et al.* used a protocol in which NPCs are driven towards a motor neuron fate, and once neuronal induction is done, astrogenesis begins (Roybon et al., 2013). For cortical astrocyte development, we took inspiration from that protocol, and added cortical neuronal induction (as described (Bell et al., 2016)) before astrogenesis, for protocols 2 and 3.

For protocol 2, when NPCs reached 50-60% confluence, they were placed in neuron differentiation media (Brainphys, N2, B27, GDNF and BDNF). There was a half-media change on the cells every 2-3 days, but the cells were not split. At the end of three weeks of neuronal differentiation, the cells were split, and replated on Matrigel, and astrocytic differentiation began, which was identical to that of protocol 1, with ADM1 (2 weeks), ADM2 (6 weeks) and ADM3 (2 weeks).

For protocol 3, we plated NPCs on Matrigel coated dishes, and once the cells reached 60-70% confluency, we changed the media to one containing DMEM/F12, 10% FBS and 5 ug/ml of CNTF for 2 weeks. Media was changed every 2-3 days, and the cells were split once, one week into the protocol.

For all protocols, the NPCs that we used were at passage 2 or 3.

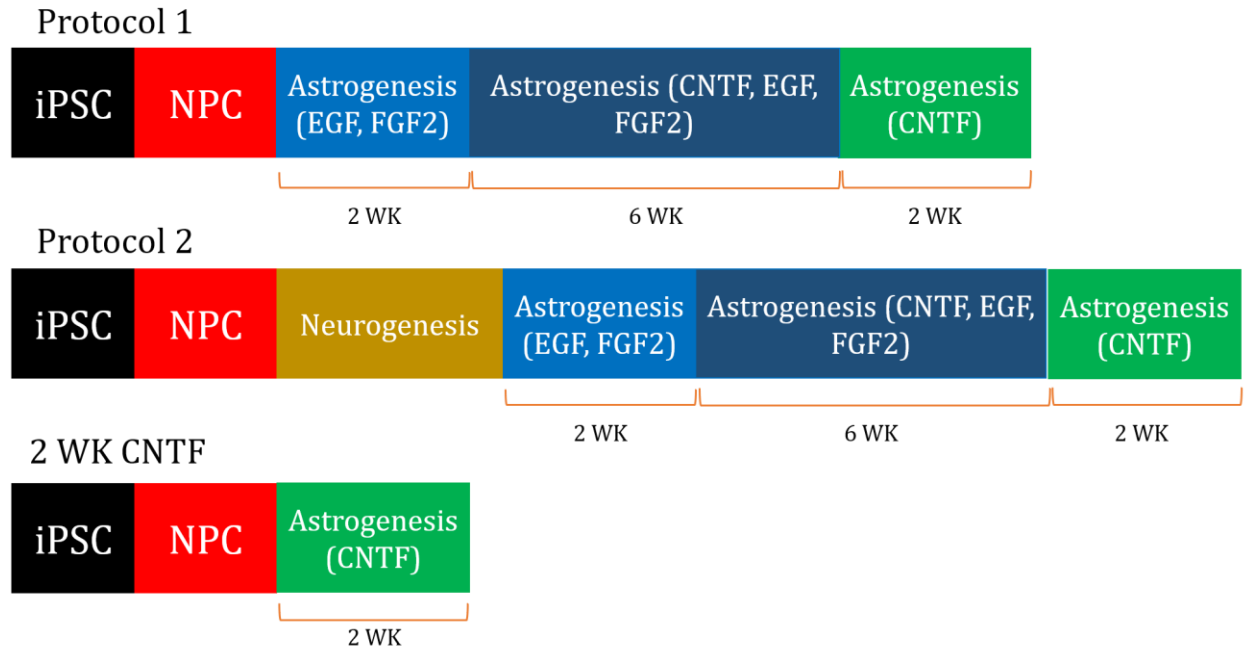


Figure 2: Overview of the different protocols. Protocol 1 – 10 weeks of astrogenesis, with three different stages: stage 1 – astrocyte differentiation media 1 (ADM1 - DMEM/F12, 10% FBS, EGF, FGF2), stage 2 – ADM2 (DMEM/F12, 10% FBS, EGF, FGF2, CNTF), stage 3 – ADM 3 (DMEM/F12, 10% FBS, CNTF). Protocol 2 – 3 weeks of neuronal differentiation (Brainphys, N2, B27, BDNF, GDNF), followed by astrogenesis identical to protocol 1 (ADM1, followed by ADM2 and ADM3). Protocol 3 – 2 weeks of astrogenesis with - DMEM/F12, 10% FBS, CNTF.

Astrocyte differentiation and maturation for ALS vs. control cell lines

For astrocytic differentiation, we used protocol 2. We used one biological replicate of 3 different cells from 3 ALS patients and their age- and sex-matched controls. The information regarding mutation, age and sex has been shown in Table 3.

Table 3. Information regarding age, sex and mutation of the patients and their age- and sex-matched controls.

Patient	Mutation	Age	Sex	Matched control	Age	Sex
Patient #1	SOD1I113T	55	Male	Subject #1	57	Male
Patient #2	SOD1I113T	59	Male	Subject #2	61	Male
Patient #3	SOD1A4V	45	Female	Subject #3	51	Female

Immunocytochemistry

We placed 12-13 coverslips into one 6 cm petri dish. Then, we coated each coverslip with Matrigel. After 30 minutes, we added DMEM/F12 and 10% FBS to dish and incubated the dishes overnight. The next day, we aspirated the media in the petri dish and plated cells from each cell line on the coated coverslips, at about 60-70% confluency. The next day, we fixed the cells on the coverslips. The cells were fixed using 4% PFA, for 15 minutes. After 3 PBS washes, we added PBS + 2% triton-x to permeabilize the cell membrane. The coverslips were then blocked for 2 hours in blocking solution, and then incubated overnight in blocking solution with primary antibody, at 4 °C. The next day, the cells were washed with PBS 3 times, and then placed in blocking solution with secondary antibody and incubated at room temperature, in the dark for 2 hours. The cells were then washed with PBS 4 times, and mounted on glass slides. The slides were left overnight at room temperature in the dark, and then transferred to freezer the next day. The primary antibodies used were GFAP (1:500, in chicken, Milipore, Cat#: AB5541), MAP2 (1:1000, in guinea pig, Synaptic Systems. Cat# 188 004), S100B (1:500, in mouse, Sigma, Cat#: S2532) and NESTIN (1:100, in mouse, ThermoFisher, Cat MA1-110). We then used the respective secondary antibodies: anti-chicken (488nm, Sigma, Cat#: SAB4600039), anti-guinea pig (568 nm, Sigma, Cat#: SAB4600080) and anti-mouse (647nm, Sigma, Cat#: SAB4600353).

RNA extraction, cDNA development and qPCR – Comparison of different protocols

Cells were extracted at the NPC stage, as well as the end of each protocol. For RNA extraction, we used the Qiagen RNeasy kit (Cat No./ID: 74106), according to manufacturer's instructions. For all samples, 1 ug of RNA was used. The RNA extracted was then reverse transcribed into cDNA, using RT-PCR kit from Qiagen (Cat No./ID: 205311), and the quantitative RT-PCR was

performed with Fast SYBR green master mix (Applied Biosystems). The sequences of qPCR primers used for mRNA quantification in this study were obtained from Integrated DNA Technologies and are shown in Table 3. The efficiency of the primers was evaluated, and only primers with efficiencies 90-110% were accepted for the purposes of our experiments. Efficiencies more than 100% for primers could mean that primers detect targets other than their specific target, and therefore they show a higher efficiency. As well, we used two housekeeping genes, RPL13A and GAPDH, which both had minimum variability in their Ct values. After 40 cycles, the Ct values were determined. To control variability between plates, we ran both housekeeping genes on every plate. For example, if we ran one sample on two separate plates, with different targets on each plate, both of those plates had RPL13A and GAPDH present. Therefore, for all samples, the target genes were normalized to two housekeeping genes, for which the values were obtained from the sample plate. To normalize the samples, the Ct value of target gene was subtracted from the Ct value of the housekeeping gene, and this value is called ΔCt . Since we had two housekeeping genes, we calculated the ΔCt between the target gene and house keeping gene and averaged of the two values. We used the average of these two ΔCt values as the final ΔCt value for each sample. $\Delta\Delta\text{Ct}$ was calculated, using ΔCt values from HFA as control, and ΔCt values obtained from each protocol for each gene were normalized to values from HFA. In short, $\Delta\Delta\text{Ct}$ was calculated for each sample by subtracting ΔCt value of HFA from ΔCt value obtained from each protocol. As well, we calculated $\Delta\Delta\text{Ct}$ comparing the values from each protocol to values obtained from NPCs. In this case, each cell line was normalized to the NPCs from the same cell line.

RNA extraction, cDNA development and qPCR – Comparison of ALS vs. control cells lines

Cell, RNA and cDNA was extracted, qPCR was carried out and data was normalized as above.

The sequences of qPCR primers used for mRNA quantification in this study were obtained from Integrated DNA Technologies and are shown in Table 3. To normalize the samples, ΔCt between target genes and each housekeeping gene was calculated, and we used the average of the two values as the ΔCt for each sample. $\Delta\Delta\text{Ct}$ was calculated, using values from healthy astrocytes as control, and values obtained from patient cell lines for each gene were normalized to values from healthy cell line astrocytes.

Statistical analysis – comparison of different protocols

Statistical analyses were performed using GraphPad 6.0. All data are presented as mean \pm SEM. The data was not normally distributed, therefore we used Kruskal-Wallis test. In the event that there is significance indicated in the Kruskal-Wallis test, with $p < 0.05$, we conducted a Dunn's post-hoc analysis test. In all cases, the significance level was established at $p < 0.05$.

For the following targets: SOX1, NESTIN, EAAT1, EAAT2, S100B, GAT3, AQP4, and KIR4.1, the values for each cell line from each protocol was compared to that of HFA. For the following targets, ALDH1L1, GS, Cx43 and MAP2, the values for each cell lines from protocol 2 and 3 were compared to that of protocol 1. The reason for not comparing ALDH1L1, GS, Cx43, and MAP2 values to HFA was that we did not have enough sample to complete that experiment for these genes. The values are presented as $\Delta\Delta\text{Ct}$ in each figure. The $\Delta\Delta\text{Ct}$ values were obtained by subtracting the stem-cell derived astrocyte values for each protocol from the human fetal astrocyte values (SOX1, NESTIN, EAAT1, EAAT2, S100B, GAT3, AQP4, and KIR4.1) or NPC values (ALDH1L1, GS, Cx43 and MAP2). Fold change was calculated as $2^{\Delta\Delta\text{Ct}}$.

Statistical analysis – ALS vs. control cell lines

Statistical analyses were performed using GraphPad 6.0. All data are presented as mean \pm SEM.

The data was not normally distributed, therefore we used the Mann-Whitney test to evaluate statistical significance between Δ Ct values of healthy controls and patient astrocytes. In all cases, the significance level was established at $p < 0.05$.

Here, we analyzed the data two ways. For one, we compared each patient cell line to its respective age- and sex-matched controls. We also pooled the control values from the male patients together, and compared each of the male patient cell lines to the pooled value. These two methods did not change the statistical significance or the direction of change in our findings.

Therefore, in Figure 13, we compared each patient cell line to its matched control. Mann-Whitney test was used for both. For each Figure, the values are presented as $\Delta\Delta$ Ct. The $\Delta\Delta$ Ct values were obtained by subtracting the patient cell line values from the control values. Fold change was calculated as $2^{\Delta\Delta\text{Ct}}$.

We use a one-tailed Mann-Whitney test for the following markers: NESTIN, EAAT2, GS, CX43, TGFB1, S100B, AQP4, and KIR4.1, because previous studies have shown that these proteins are affected in ALS (Almad et al., 2017; Bataveljic et al., 2012; Bos et al., 2006; Ghoddoussi et al., 2010; Kelley et al., 2018; Liu & Martin, 2006; Serrano et al., 2017; Taylor et al., 2016; Tripathi et al., 2017). Therefore, we hypothesized that the levels of NESTIN, EAAT2 and KIR4.1 will be lower, and the levels of GS, CX43, S100B, AQP4, ALDH1L1 and TGFB1 will be higher in astrocytes derived from ALS patients compared to healthy controls. For all other markers, we used two tailed Mann-Whitney test because these markers have not been previously investigated in ALS.

Table 3. The sequence of forward and reverse primers, and their respective optimal conditions and efficiencies are shown here.

Species	Primer	Sequence	[]	°C	Efficiency
Human	RPL13A	Fwd: TGTTTGACGGCATCCCAC Rev: CTGTCCTGCCTGGTACTTC	600	60	90%
Human	GAPDH	Fwd: ACATCGCTCAGACACCATG Rev: TGTAGTTGAGGTCAATGAAGGG	300	60	95%
Human	SOX2	Fwd: TACAGCATGATGCAGGACCA Rev: CCGTTCATGTAGGTCTGCGA	600	60	100%
Human	NESTIN	Fwd: AAGACTTCCCTCAGCTTTCAG Rev: AGCAAAGATCCAAGACGCC	400	62	105%
Human	GS	Fwd: CAAGCAGGTGTACATGTCC Rev: CGAAATTCCTCAGGCAAC	600	60	93%
Human	S100B	Fwd: CAGCAAGGAGACCAGGAAG Rev: TGGAAAACGTGCGATGAGGG	300	60	101%
Human	EAAT1	Fwd: CCATGTGCTTCGGTTTTGTG Rev: AATCAGGAAGAGAATACCCACG	300	62	106%
Human	EAAT2	Fwd: CCAACAGAGATCAGCC Rev: ATGCTGGGAGTCAATGGTATC	600	60	92%
Human	ALDH1L1	Fwd: GTACAACCGCTTCCTCTTCC Rev: TTGATCTTGGCTGTCTCCTTC	600	60	107%
Human	MAP2	Fwd: ATCAAATGGTCCACTAGGCG Rev: CCTTGGCTTTTGTCTTGGATG	300	60	109%
Human	Kir4.1	Fwd: GCTACGGAGACCCTGAAAAG Rev: GAGGAAAAGAGACCAGAGGAATG	600	60	109%
Human	GAT3	Fwd: CTACCTGTGCTACAAGAACGG Rev: ACACGTAATGCCACCTTCAC	600	60	96%
Human	AQP4	Fwd: CATGAGTGACAGACCCACAG Rev: GAGTCCAGACCCCTTTGAAAG	300	62	99%
Human	CX43	Fwd: AAGTACCAAACAGCAGCGGA Rev: TGGGCACCACTCTTTTGCTTA	600	60	101%
Human	TGF-B1	Fwd: GCCTTTCCTGCTTCTCATGG Rev: TCCTTGCGGAAGTCAATGTAC	300	62	91%

**Chapter 3 – Evaluating the expression of NPC, astrocytic and neuronal markers in
astrocytes derived from three protocols**

Results

Astrocytes derived from all protocols are similar in mRNA expression of select NPC, astrocytic and neuronal markers to HFA.

First, we developed astrocytes from NPCs using all three protocols, from three cell lines derived from healthy subjects (2 males and 1 female). Protocol 1 was developed by our colleagues, and it is very similar to other protocols published to date (Krencik & Zhang, 2011; Serio et al., 2013; Shaltouki et al., 2013), and incorporates 10 weeks of astrogenesis. The first two weeks, we add growth factors EGF and FGF2, to promote proliferation and initial differentiation. Then, for six weeks, we add EGF, FGF2 and CNTF, in order to further differentiate the cells towards astrocytes. For the final two weeks, we add only CNTF to the media, in order to induce further maturation of astrocytes and decrease proliferation. Protocol 2 incorporates a three-week period of neuronal differentiation, after which astrogenesis starts identical to protocol 1. In protocol 3, we only added CNTF for two weeks. Once the cells reach the end of each protocol, their RNA is extracted. As shown in Figure 3, using qPCR, we assessed the mRNA expression of two NPC markers (NESTIN and SOX1), nine astrocytic markers (EAAT1, EAAT2, S100B, AQP4, GAT3, KIR4.1, CX43, ALDH1L1 and GS), and one neuronal marker (MAP2), in astrocytes derived from each protocol, in three cell lines. To verify that the cells were no longer NPCs, the mRNA levels of NESTIN and SOX1 from astrocytes from all three protocols are compared to that of HFA, as shown in Figure 3. Using the Kruskal-Wallis test, we found that there was no statistically significant difference in the expression of NESTIN ($P = 0.1426$, Figure 3A) or SOX1 ($P = 0.2420$, Figure 3B) mRNA levels when comparing astrocytes from any of the three protocols, to HFA.

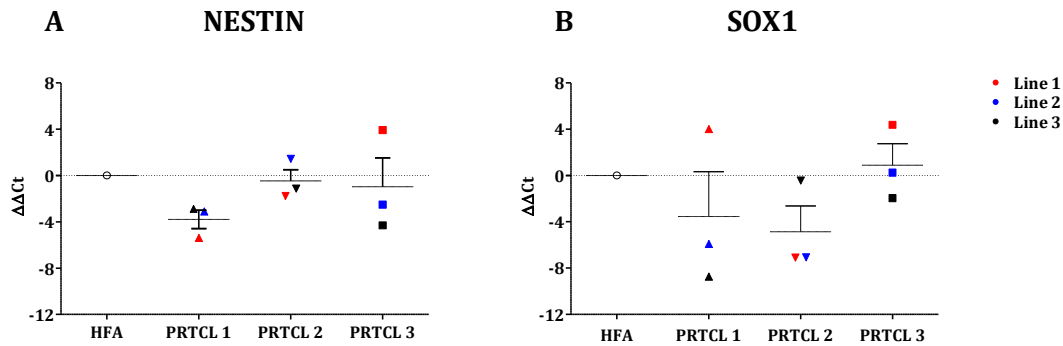


Figure 3. mRNA levels of NPC markers are not different between astrocytes derived from protocol 1, 2 and 3, compared to human fetal astrocytes (HFA). Astrocytes were derived from NPCs using protocol 1, 2, and 3, from three healthy human cell lines (line 1 and 2 are from males and line 3 is from a female) and RNA was extracted at the end of each protocol. Using qPCR, mRNA levels of NPC markers NESTIN (panel A) and SOX1 (panel B) were quantified in these astrocytes and compared to mRNA levels of NPC markers in one human fetal astrocyte line. Using the Kruskal-Wallis test, we found no statistically significant difference in NPC marker mRNA levels of stem-cell derived astrocytes from three protocols vs. HFA (Nestin: $p = 0.2197$, SOX1, $p = 0.3751$). Data is presented as mean \pm SEM. Significance is considered when $p < 0.05$.

Next, we assessed the mRNA expression levels of astrocytic markers. We compared the astrocytes from all three protocols to HFA, for the following markers: EAAT1, EAAT2, S100B, AQP4, KIR4.1 and GAT3, as shown in Figure 4. For EAAT1 mRNA expression, there is an overall effect of protocol ($p = 0.0174$), and protocol 2 has significantly lower EAAT1 mRNA levels compared to HFA. The difference in EAAT1 mRNA levels is not different in the other two protocols compared to HFA. There is also an overall effect of protocol in EAAT2 mRNA expression as well ($p = 0.0422$). However, EAAT2 mRNA expression is only significantly lower in astrocytes developed from protocol 1 vs. HFA ($p < 0.05$). The mRNA expression of S100B, AQP4, KIR4.1 and GAT3 are not different in astrocytes derived from the three protocols vs. HFA. However, these genes were easily detected via qPCR, meaning that they were expressed abundantly at the mRNA level.

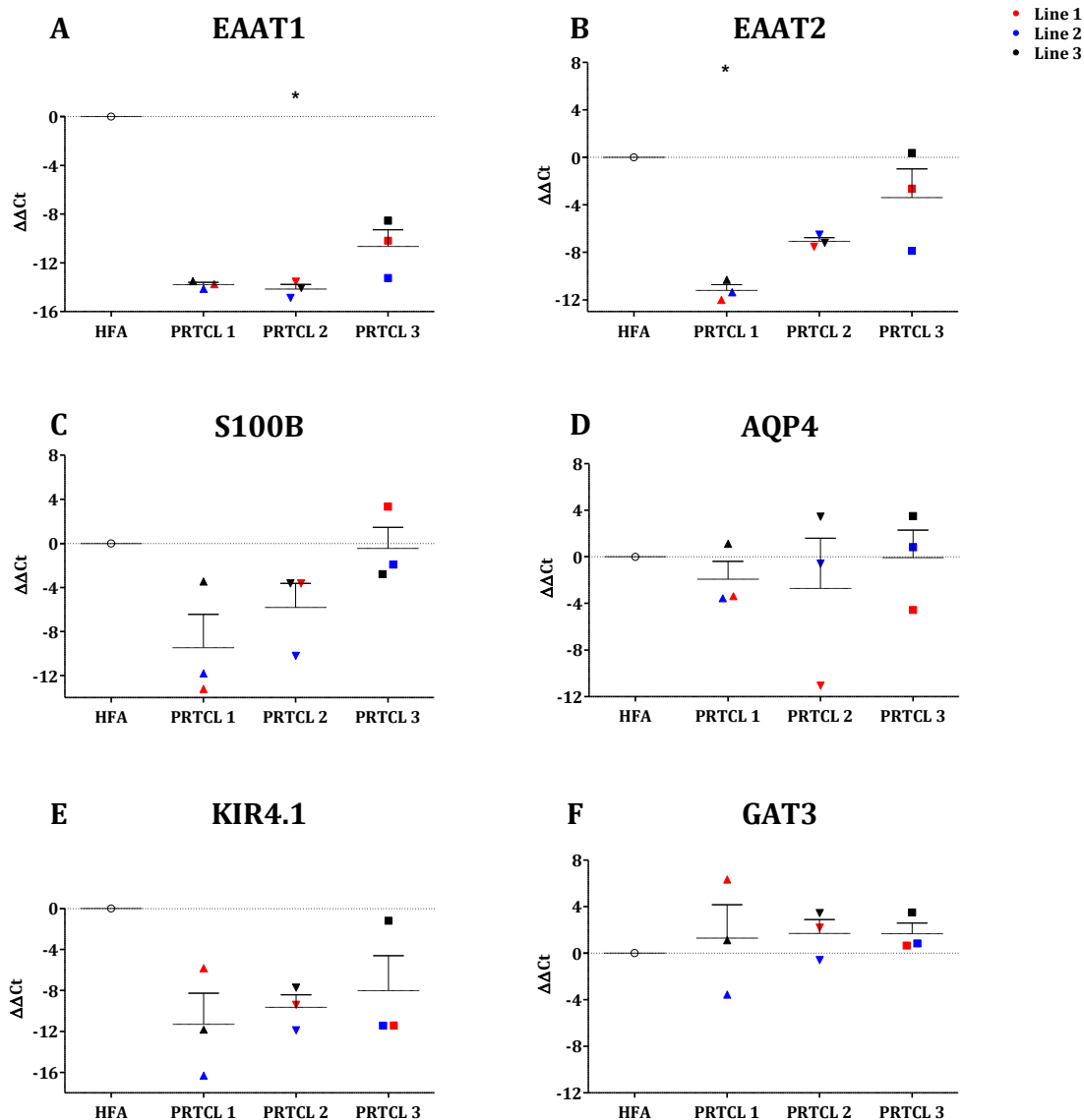


Figure 4. mRNA levels of astrocytic markers are not different in astrocytes derived from protocol 1, 2 and 3, compared to human fetal astrocytes (HFA). Astrocytes were derived from NPCs using protocol 1, 2, and 3, from three healthy human cell lines (line 1 and 2 are from males and line 3 is from a female) and RNA was extracted at the end of each protocol. Using qPCR, mRNA levels of astrocytic markers were quantified in these astrocytes and compared to mRNA levels of astrocytic markers in one human fetal astrocyte line. A: EAAT1 mRNA expression – astrocytes from protocol 2 had significantly lower EAAT1 levels ($p = 0.0174$). EAAT1 mRNA levels were not different in protocol 1 and 2 vs. HFA. B: EAAT2 mRNA expression - astrocytes from protocol 1 had significantly lower EAAT2 levels ($p = 0.0422$) vs. HFA. mRNA expression of S100B (panel C, $p = 0.0805$), AQP4 (panel D, $p = 0.9365$), KIR4.1 (panel E, $p = 0.3751$) and GAT3 (panel F, $p = 0.8538$) were not different in any of the protocols vs. HFA. Kruskal-Wallis test was used, followed by Dunn’s post hoc analysis between the pairs. Data is presented as mean \pm SEM. Significance is considered when $p < 0.05$. “*” represents statistically significant difference between a given protocol and HFA.

We also measured the mRNA levels of other astrocytic markers, ALDH1L1, GS and CX43, as well as a neuronal marker, MAP2. For these markers, we compared protocol 2 (3 weeks of neurogenesis and 10 weeks of astrogenesis) and protocol 3 (2 weeks of CNTF) to protocol 1, as shown in Figure 5 and Figure 6. The reason for not including HFA in these comparisons is that we did not have enough material to complete qPCR experiments and measure the mRNA levels of these four genes. The mRNA levels of ADH1L1, GS and Cx43 were not different between the three different protocols (Figure 5). Further, the mRNA levels of neuronal marker MAP2 were also not different between the three different protocols (Figure 6). We evaluated the mRNA expression of MAP2 to characterize the NPCs more thoroughly.

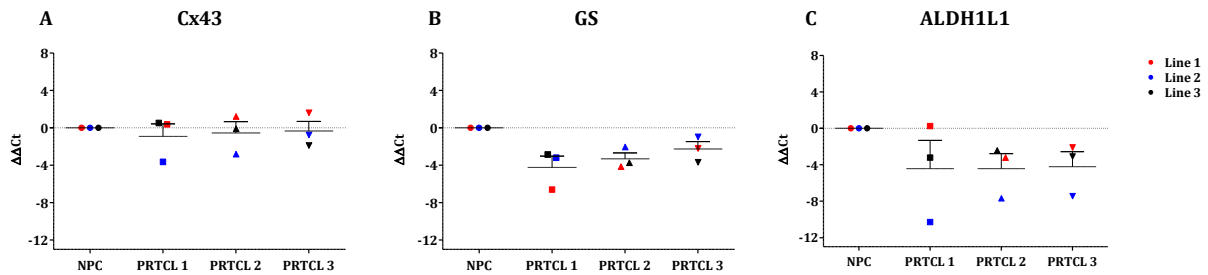


Figure 5. mRNA levels of astrocytic markers are not different in astrocytes derived from protocol 2 and 3, compared to protocol 1. Astrocytes were derived from NPCs using protocol 1, 2, and 3, from three healthy human cell lines (line 1 and 2 are from males and line 3 is from a female) and RNA was extracted at the end of each protocol. Using qPCR, mRNA levels of astrocytic markers were quantified in these astrocytes and mRNA levels of astrocytic markers in astrocytes from protocol 2 and 3 were compared to mRNA levels of astrocytic markers in astrocytes from protocol 1. mRNA expression of GS (panel A, $p = 0.3051$), Cx43 (panel B, $p = 0.8763$) and ALDH1L1 (panel C, $p = 0.9834$) were not different between the three protocols. Kruskal-Wallis test was used, followed by Dunn's post hoc analysis between the pairs. Data is presented as mean \pm SEM. Significance is considered when $p < 0.05$.

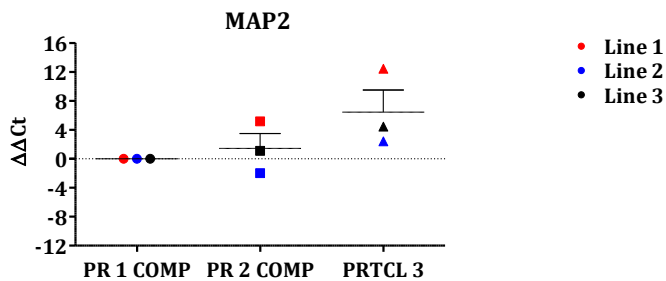


Figure 6. mRNA levels of neuronal marker MAP2 is not different in astrocytes derived from protocol 2 and 3, compared to protocol 1.

Astrocytes were derived from NPCs using protocol 1, 2, and 3, from three healthy human cell lines (line 1 and 2 are from males and line 3 is from a female) and RNA was extracted at the

end of each protocol. Using qPCR, mRNA levels of neuronal MAP2 was quantified in these astrocytes and mRNA levels of neuronal astrocytes from protocol 2 and 3 were compared to mRNA levels of neuronal markers in astrocytes from protocol 1. mRNA expression of MAP2 was not different between the three protocols ($p = 0.1385$). Kruskal-Wallis test was used, followed by Dunn's post hoc analysis between the pairs. Data is presented as mean \pm SEM. Significance is considered when $p < 0.05$.

Astrocytes derived from all protocols are similar in mRNA expression to NPCs.

Next, we compared mRNA expression of the above-mentioned markers between astrocytes derived from each protocol and NPCs. Astrocytes from each cell line were compared to their respective NPC lines. As shown in Figure 7, NPC markers are not different in astrocytes derived from protocols 1, 2 and 3 compared to NPCs.

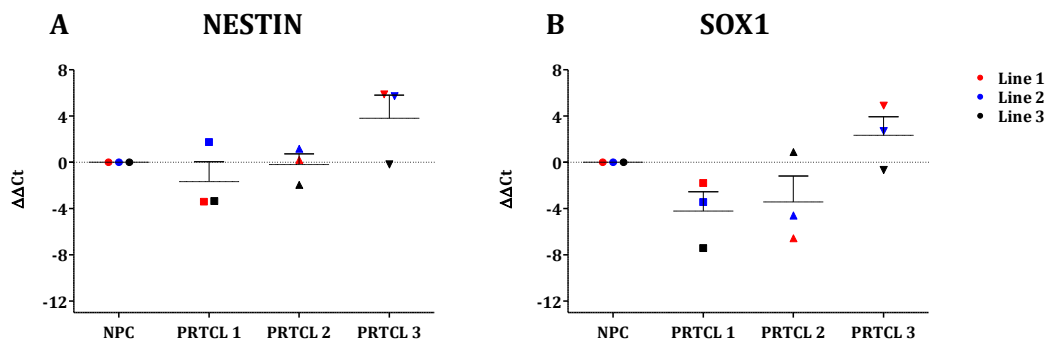


Figure 7. mRNA levels of NPC markers are not different between astrocytes derived from protocol 1, 2 and 3, compared to NPCs. Astrocytes were derived from NPCs using protocol 1, 2, and 3, from three healthy human cell lines (line 1 and 2 are from males and line 3 is from a female) and RNA was extracted at the end of each protocol. Using qPCR, mRNA levels of NPC markers NESTIN (panel A, $p = 0.4529$) and SOX1 (panel B, $p = 0.1246$) were quantified in these astrocytes and compared to mRNA levels of NPC markers in NPCs. Each cell line was compared to its own NPC. Using Kruskal-Wallis test, we found no statistically significant difference between mRNA levels of stem-cell derived astrocytes from three protocols vs. their respective NPCs. Data is presented as mean \pm SEM. Significance is considered when $p < 0.05$.

For astrocytic marker expression also, there was no significant difference in astrocytes derived from the three protocols vs. NPCs. More specifically, although the Kruskal-Wallis test indicated that there was an effect of protocol on mRNA expression of EAAT1 ($p = 0.0412$), EAAT2 ($p = 0.0311$), and S100B ($p = 0.0384$), Dunn's post hoc analysis did not indicate any significant difference in astrocytes derived from any of the protocols compared to their NPCs (Figure 8 and 9). For neuronal marker MAP2 mRNA expression, although there was a significant effect of protocol ($p = 0.0422$), the post hoc analysis did not indicate any significant difference between astrocytes derived from the protocols and NPCs (Figure 10). The reason for the lack of significant difference may be due to a type II statistical error, meaning there is a difference that the statistical test renders not significant, because the number of samples in the experiments is only 3. However, the lack of difference may also be due to the fact that there were no changes in mRNA expression of the selected markers in the cells upon undergoing the different protocols. In order to distinguish between the two, we need to increase the number of samples.

There is a heterogeneous population of cells in cultures developed from protocol 1 and 2, including astrocytes, NPCs and neurons.

The cells that underwent protocol 1, 2 and 3, as well as NPCs, were stained with astrocytic, NPC and neuronal markers, to distinguish between different populations of cells. This experiment will compliment our data from qPCR data, because when collecting RNA for qPCR, we collect and analyze the RNA from all cells in the dish. Therefore, the data that we get is the average mRNA expression across all cells.

At the NPC stage, cells were imaged for GFAP (astrocytic marker), NESTIN (NPC marker) and MAP2 (neuronal marker). As shown in Figure 11A, the cells have a typical NPC morphology, with small processes. As well, GFAP, NESTIN and MAP2 are expressed in all of the cells in the

image. GFAP and NESTIN are both abundantly expressed in NPCs. Further, MAP2 protein expression has been shown in NPCs at low levels (Mohammad, Al-Shammari, Al-Juboory, & Yaseen, 2016), and its expression increases as NPCs develop towards neurons.

For all astrocyte cultures, we imaged GFAP (astrocytic and NPC marker), MAP2 (neuronal marker) and S100B (astrocytic marker). For protocol 1, as shown in Figure 11B, astrocytes expressed GFAP, which is expressed in both astrocytes and NPCs. MAP2 staining showed a neuron, indicating that there are some neurons in the culture as well. Further, in panel B, S100B staining is expressed highly in one cell, while the other GFAP-positive cells did not express S100B. These cells may be NPCs that have not yet matured towards an astrocytic fate. Therefore, we can conclude that there is a heterogeneous population of cells in the culture, including astrocytes, neurons, and NPCs.

Next, we imaged cultures that underwent protocol 2 (3 weeks of neurogenesis and 10 weeks of astrogenesis), with the same markers: GFAP, MAP2 and S100B. As shown in Figure 11C, the cells express GFAP and S100B, however, some cells express GFAP but not S100B. Similar to cultures from protocol 1, the cells that are GFAP-positive and S100B-negative may be at the NPC stage, not yet developed into an astrocyte. Further, MAP2 staining shows faint staining of \ neuron. In the cultures using protocol 2, similar to protocol 1, there is a heterogeneous population of cells in the culture, although S100B is expressed in more cells and the MAP2 staining is weaker.

Finally, we stained cells that underwent protocol 3 (2 weeks of CNTF), and morphologically they look similar to NPCs. Further, they express GFAP, MAP2 and S100B. However, S100B staining is weaker in these cells and all cells show MAP2 staining. Considering cell morphology

and protein expression, these cells may be at the NPC stage, and may not be considered as astrocytes.

Figure 12 shows astrocytic morphology of astrocytes derived from protocols 1 and 2.

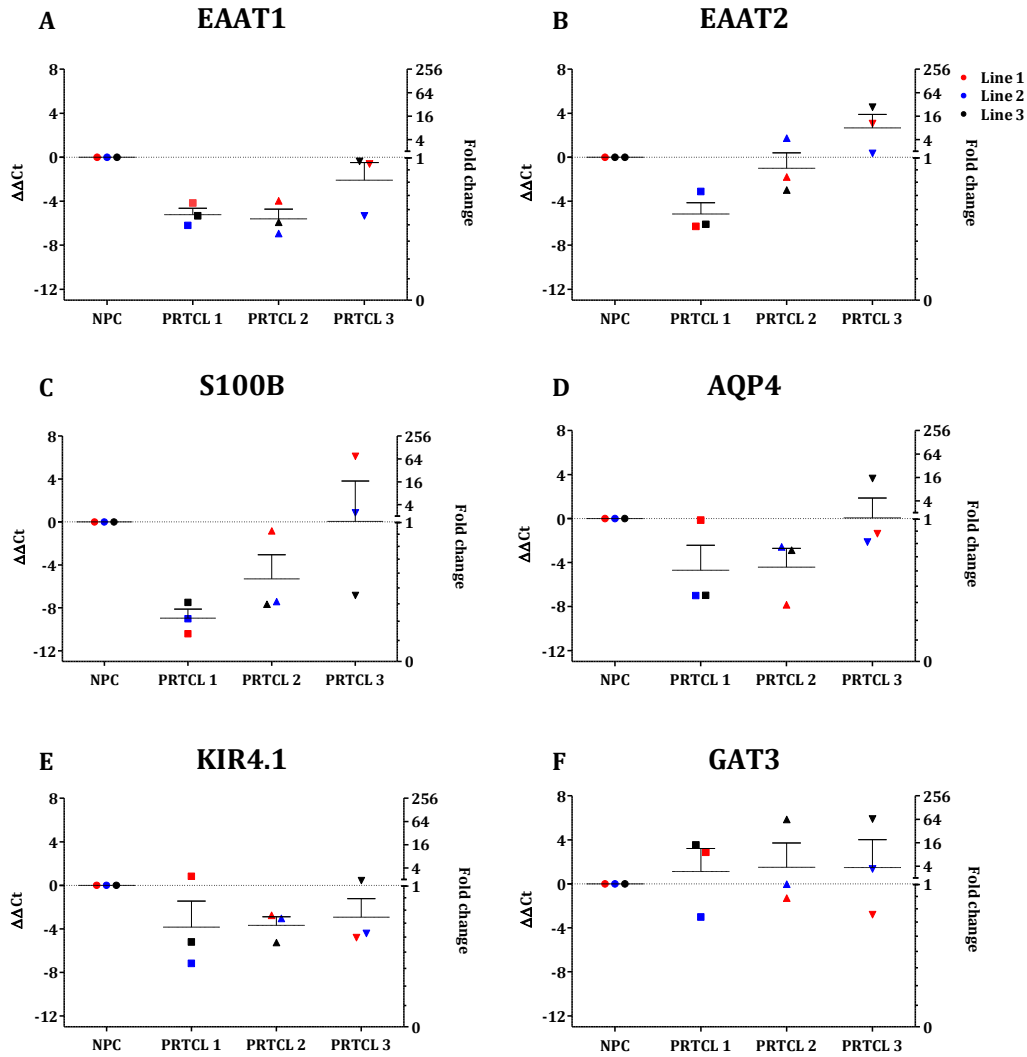


Figure 8. mRNA levels of astrocytic markers are not different in astrocytes derived from protocol 1, 2 and 3, compared to NPCs. Astrocytes were derived from NPCs using protocol 1, 2, and 3, from three healthy human cell lines (line 1 and 2 are from males and line 3 is from a female) and RNA was extracted at the end of each protocol. Using qPCR, mRNA levels of astrocytic markers were quantified in these astrocytes and compared to mRNA levels of astrocytic markers in NPCs. Each cell line was compared to its own NPC. Although there was a significant effect of protocol in EAAT1 ($p = 0.0412$), EAAT2 ($p = 0.0311$), and S100B ($p = 0.0384$) mRNA expression, there was no difference in mRNA expression of EAAT1 (panel A), EAAT2 (panel B), S100B (panel C), AQP4 (panel D, $p = 0.0688$), KIR4.1 (panel E, $p = 0.5098$) and GAT3 (panel F, $p = 0.9626$) in astrocytes derived from different protocols, compared to their respective NPCs. Kruskal-Wallis test was used, followed by Dunn's post hoc analysis between the pairs. Data is presented as mean \pm SEM. Significance is considered when $p < 0.05$. “*” represents statistically significant difference between a given protocol and HFA.

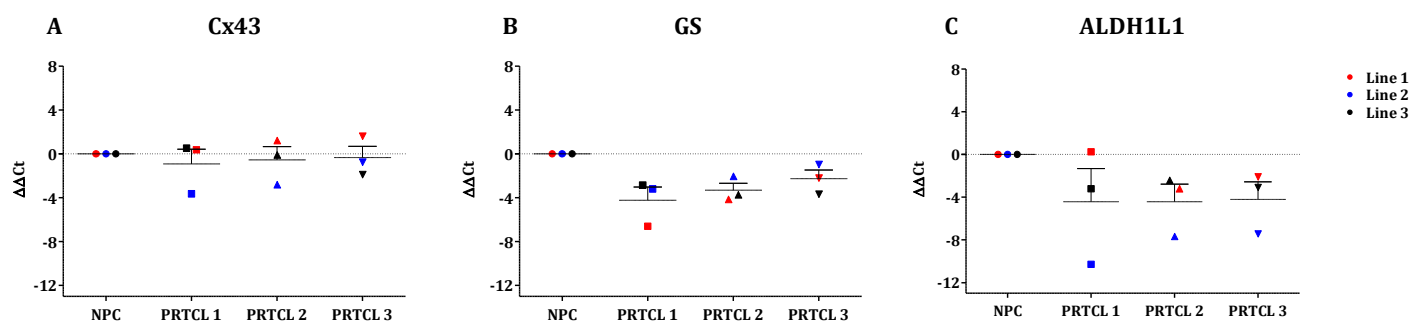


Figure 9. mRNA levels of astrocytic markers are not different in astrocytes derived from protocol 1, 2 and 3, compared to NPCs. Astrocytes were derived from NPCs using protocol 1, 2, and 3, from three healthy human cell lines (line 1 and 2 are from males and line 3 is from a female). Using qPCR, mRNA levels of astrocytic markers were quantified in these astrocytes and compared to mRNA levels of astrocytic markers in NPCs. Each cell line was compared to its own NPC. mRNA expression of CX43 (panel A, $p = 0.9880$), GS (panel B, $p = 0.0627$) and ALDH1L1 (panel C, $p = 0.2638$) were not different in the three protocols vs. their respective NPCs. Kruskal-Wallis test was used, followed by Dunn’s post hoc analysis between the pairs. Data is presented as mean \pm SEM. Significance is considered when $p < 0.05$.

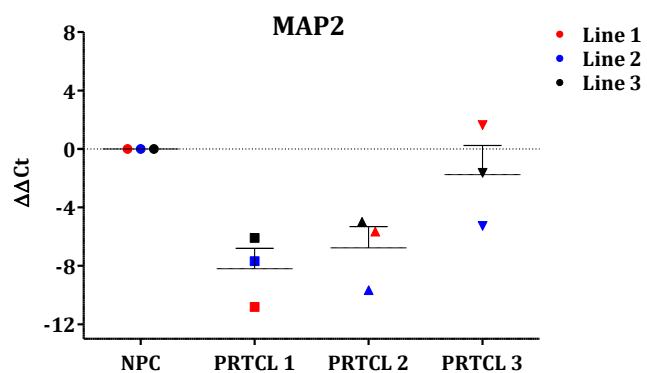


Figure 10. mRNA levels of neuronal marker MAP2 is not different in astrocytes derived from protocol 1, 2 and 3, compared to NPCs. Astrocytes were derived from NPCs using protocol 1, 2, and 3, from three healthy human cell lines (line 1 and 2 are from males and line 3 is from a female). Using qPCR, mRNA levels of neuronal marker MAP2 was quantified in these astrocytes and compared to mRNA levels of MAP2 markers in NPCs. Each cell

line was compared to its own NPC. Although there was a main effect of protocol ($p = 0.0422$), mRNA expression of MAP2 was not different in the three protocols vs. their respective NPCs. Kruskal-Wallis test was used, followed by Dunn’s post hoc analysis between the pairs. Data is presented as mean \pm SEM. Significance is considered when $p < 0.05$

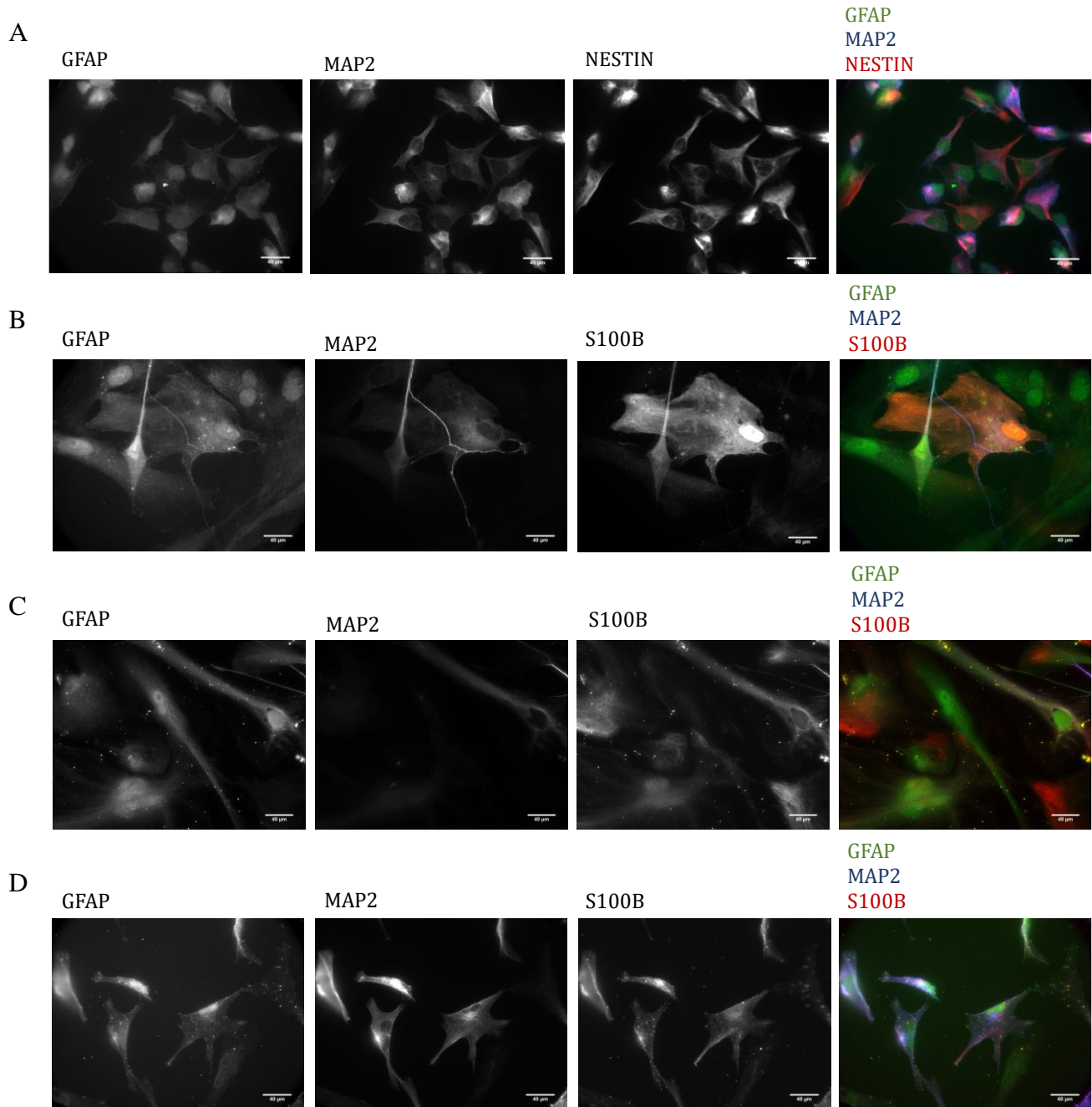


Figure 11. Cultures from protocol 1 and 2 have a heterogeneous population of cells, including astrocytes, neurons and NPCs, while cultures from protocol 3 mostly resemble NPCs. A: NPCs, scale bar 40 µm, from left to right, cells stained with GFAP, MAP2 and NESTIN. Final figure is a composite of all three, where GFAP is green, MAP2 is blue and NESTIN is red. **B:** astrocytes derived from NPCs, using the protocol with 10 weeks of astrogenesis, **C:** astrocytes derived from NPCs, using the protocol with 3 weeks of neurogenesis and 10 weeks of astrogenesis, **D:** astrocytes derived from NPCs, using the protocol with 2 weeks of astrogenesis, scale bar 40 µm, from left to right, cells stained with GFAP, MAP2 and S100B. Final figure is a composite of all three, where GFAP is green, MAP2 is blue and S100B is red.

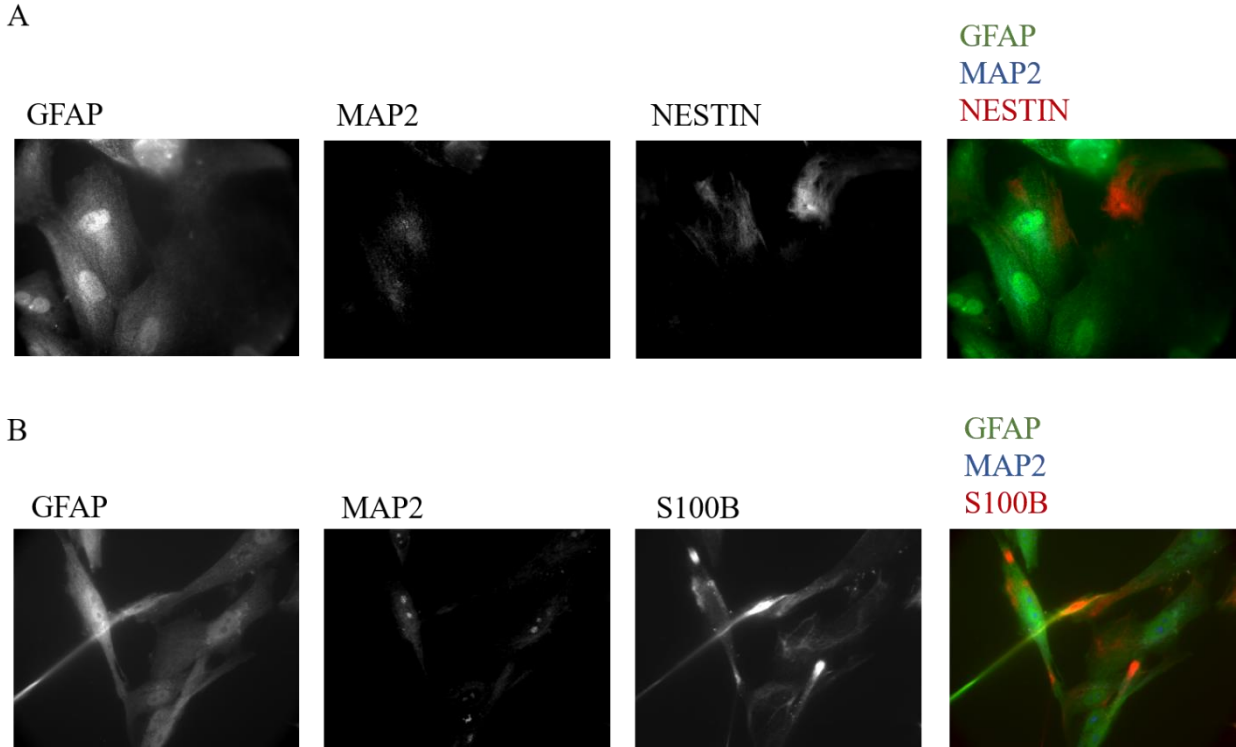


Figure 12. Cultures from protocol 1 and 2 show astrocytic morphology. A: astrocytes derived from NPCs, using the protocol with 10 weeks of astrogenesis, B: astrocytes derived from NPCs, using the protocol with 3 weeks of neurogenesis and 10 weeks of astrogenesis, scale bar 40 μ m, from left to right, cells stained with GFAP, MAP2 and NESTIN (A) and S100B (B). Final figure is a composite of all three, where GFAP is green, MAP2 is blue and S100B and NESTIN are red.

Chapter 4 – characterization of astrocytes derived from stem cells of patients with amyotrophic lateral sclerosis

Results

Stem-cell derived astrocytes express changes previously observed in other ALS models.

Astrocytes were derived from NPCs, using a protocol that incorporated 3 weeks of neurogenesis and 10 weeks of astrogenesis. We have previously shown that these astrocytes express astrocytic markers at the mRNA and protein level (Figure 4, 5 and 11). Here, we evaluated the mRNA levels of one NPC marker (NESTIN), nine astrocytic markers (EAAT1, EAAT2, S100B, AQP4, KIR4.1, GAT3, GS, Cx43 and ALDH1L1) and one cytokine (TGFB1) in astrocytes derived from 3 ALS patients with SOD1 mutations (2 SOD1I113T and 1 SOD1A4V) compared to their age- and sex-matched controls.

We found that the mRNA levels of S100B, AQP4, EAAT1, GAT3 and KIR4.1 did not change in ALS astrocytes compared to healthy controls. However, we found that mRNA levels of NESTIN and EAAT2 were lower and mRNA levels of GS, Cx43, and TGFB1 were higher in ALS astrocytes compare to healthy controls ($p < 0.05$).

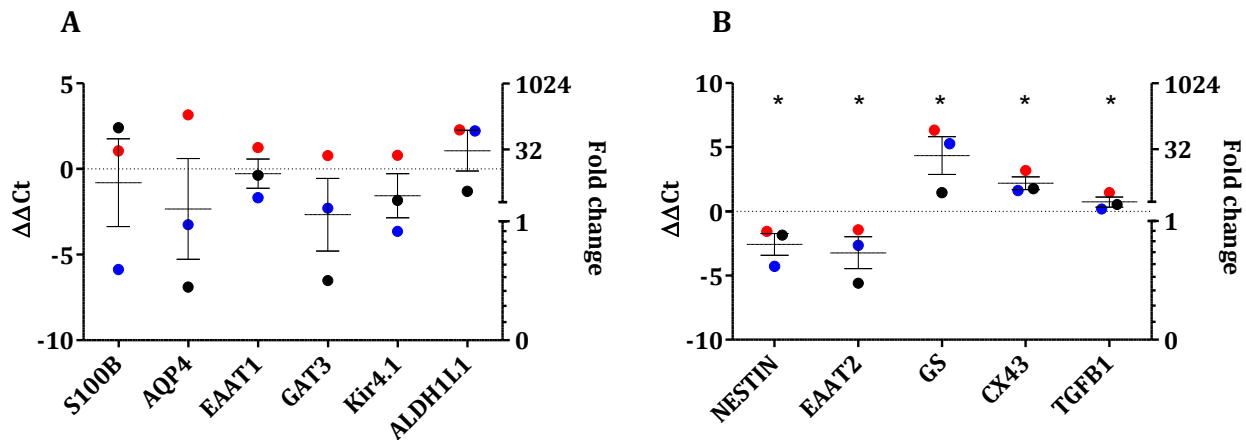


Figure 13. ALS astrocytes show ALS phenotypes in their mRNA expression. Astrocytes were derived from NPCs, using three cell lines from ALS patients with SOD1 mutation and their age- and sex-matched controls (line 1 and 2 are from males (black and blue, respectively) and line 3 is from a female (red)). Using qPCR, mRNA levels NPC marker NESTIN, astrocytic markers and an inflammatory cytokine was quantified in ALS astrocytes and compared to mRNA levels in healthy astrocytes. Each ALS cell line was compared to its matched control. Panel A: there was no significant difference in mRNA expression of S100B, AQP4, EAAT1, GAT3, KIR4.1 and ALDH1L1. Panel B: mRNA levels of NESTIN ($p < 0.05$) and EAAT2 ($p < 0.05$) were lower, and mRNA levels of GS ($p < 0.05$), Cx43 ($p < 0.05$), and TGFB1 ($p < 0.05$) were higher in ALS astrocytes compared to their matched healthy controls. Mann-Whitney test was used to evaluate statistical significance. Data is presented as mean \pm SEM. Significance is considered when $p < 0.05$.

Chapter 5 – Discussion, conclusions, limitations and future directions

Discussion

In the first aim of this study, we attempted to evaluate the maturity of stem cell-derived astrocytes using three different protocols, as they compared to HFA, based on astrocytic marker mRNA and protein expression. Since there is no golden standard accepted to identify mature astrocytes, and HFA are also not mature, we did not have exact characteristics to consider for these cells. As shown in Table 6, we found that astrocytes derived from all three protocols had similar astrocytic marker mRNA expression to HFA. Therefore, we may conclude that although these astrocytes may not be fully mature, they do have astrocytic features, which is also confirmed by their expression of astrocytic protein S100B.

Table 6. mRNA expression of astrocytic markers in stem-cell derived astrocytes from all three protocols is similar to human fetal astrocytes.

	PRCL 1	PRCL 2	PRCL 3
NESTIN	No change	No change	No change
SOX1	No change	No change	No change
EAAT1	No change	↓	No change
EAAT2	↓	No change	No change
S100B	No change	No change	No change
GAT3	No change	No change	No change
AQP4	No change	No change	No change
KIR4.1	No change	No change	No change

Astrocytes derived from protocol 1, which incorporated 10 weeks of astrogenesis, had lower mRNA levels of the glutamate transporter EAAT2, compared to HFA. EAAT2 is an astrocyte-specific marker, and its expression begins at about 20 weeks gestation and increases as astrocytes mature in humans (Roybon et al., 2013). Since EAAT2 expression is significantly lower in astrocytes derived from protocol 1, these astrocytes may not be as mature as HFA. However,

these findings are from one biological replicate of each line. Indeed, there is cell line to cell line variation, and there is also variation between different batches of the same cell line. Therefore, it is important to confirm observations in more biological replicates in order to make any conclusive remarks. Further, these astrocytes express NPC markers at the protein and mRNA level, although their expression is expected to decrease as astrocytes mature. Therefore, we concluded that these astrocytes may not be fully mature. Although immature astrocytes are a valuable system to study diseases in, for diseases with adult onset (such as ALS, with average onset at 45-60 years), mature astrocytes may be more applicable.

In order to achieve astrocytic maturity, we created a protocol that more closely emulated astrogenesis *in vivo*. During development, astrogenesis occurs after neurogenesis, and once the neurons develop they support and stimulate astrogenesis by releasing factors such as cardiotrophin-1 (Barnabé-Heider et al., 2005). In order to achieve spinal astrocyte maturity, Roybon *et al.* used a protocol in which NPCs are driven towards a motor neuron fate, and once neuronal induction is done, astrogenesis begins (Roybon et al., 2013). For cortical astrocyte development, we took inspiration from that protocol, and added cortical neuronal induction (as described (Bell et al., 2016)) before astrogenesis (protocol 2). When evaluating the mRNA levels of astrocytic markers, these astrocytes had similar levels of all of markers, other than EAAT1, which was lower in these astrocytes compare to HFA. In rodents, EAAT1 levels decrease as astrocytes mature. Therefore, the lower EAAT1 levels in these astrocytes, compared to HFA, does not necessarily mean that these astrocytes are less mature. Interestingly, although not statistically significant, astrocytes from protocol 1 also had lower levels of EAAT1. Further, astrocytes from protocols 1 and 2 expressed S100B at the protein level as well.

When we compared the mRNA levels of astrocytic markers in astrocytes derived from protocols 1 and 2 to NPCs, surprisingly, we found that astrocytes from all protocols had similar levels of all markers compared to the NPCs. Therefore, we hypothesize that the NPCs may be further along astrocytic differentiation, and may be astrocyte progenitor cells. Since the NPCs in this study expressed mRNA of astrocytic markers, we decided to treat them with CNTF alone for two weeks (protocol 3). CNTF, a cytokine from the IL-6 family, induces differentiation of cerebral cortical precursor cells into astrocytes and inhibits their neuronal differentiation (Shaltouki et al., 2013). In fact, most protocols incorporate CNTF treatment at the end of astrogenesis to induce terminal differentiation (Krencik, Weick, Liu, Zhang, & Zhang, 2011; Serio et al., 2013; Shaltouki et al., 2013). Although the astrocytic marker expression of the cells derived from protocol 3 was similar to HFA and the other two protocols, the morphology of these astrocytes looked more similar to NPCs. It is important to note that although mRNA levels of proteins can provide insight into the presence of these proteins, mRNA does not always accurately translate to protein. There are post-translational modifications that may change as astrocytes mature, therefore changing the protein levels of certain astrocyte markers, although mRNA levels of these markers may remain the same. Further, NPCs from the fetal or adult brain have not been thoroughly characterized for astrocytic markers. Future studies investigating the expression of astrocytic marker mRNA in fetal and adult NPCs is warranted to help us understand the development stage of the stem cell-derived NPCs.

In order to evaluate the astrocyte cultures derived from different protocols, we also measured the mRNA levels of NPC markers (NESTIN and SOX1) and a neuronal marker (MAP2). The cultures from all protocols expressed NPC and neuronal markers. When we stained the cultures with astrocytic, NPC and neuronal marker, we found that the cultures consisted of a

heterogeneous population of NPCs, astrocytes and neurons, across all three protocols. Indeed, this contributes to the variability observed in cultures from the same cell lines in different batches, as well as the cell line to cell line variability, which is a limitation of stem-cell derived cultures and dissociated cultures in general. Furthermore, it is important to note that rodent astrocytes express MAP2 (Charrigre-bertrand, Garner, Tardy, & Nunez, 1991) and MAP2 expression increases when astrocytes are activated (Charrigre-bertrand et al., 1991). Therefore, it may not be entirely surprising that astrocyte cultures express MAP2 at the mRNA and protein level.

Another limitation of cells derived from stem cells is their lack of maturity. Specifically for astrocytes, as discussed before, there is no definite marker that ensures astrocyte maturity. For example, typical markers used to identify astrocytes, such as GFAP, are highly expressed in NPCs and not expressed in astrocytes from certain regions of the brain, such as the cortex. Therefore, using GFAP as a marker for astrocytes may be misleading. Indeed, since NPCs express GFAP, quantifying mRNA levels of GFAP does not provide clear evidence of astrocyte development and maturity. Moreover, other astrocytic markers such as EAAT1 may be present in astrocytes, but not fully distinguish mature from immature astrocytes. Further, beyond marker expression, the functional capacity of cells is important. For example, if a population of astrocytes express GFAP and S100B, but cannot take up glutamate efficiently or respond to inflammatory signals appropriately, then their use in disease modeling experiments will be limited. Therefore, it is important to incorporate functional capacity in determining astrocyte maturity. Indeed, several studies evaluating stem-cell derived astrocyte maturity have shown glutamate uptake capacity, spontaneous calcium waves, transient calcium waves in response to gliotransmitters, and activation in response to inflammatory molecules, as shown in Table 2.

Although information regarding astrocyte markers and function is growing, there is little known about adult human astrocytes specifically. It has been shown that adult astrocytes differ in marker expression and morphology compared to adult mouse astrocytes as well as HFA (Zhang et al., 2016). However, the exact differences are still not completely defined. For example, *Zhang et al.*, found mRNA Cx43 to be exclusively expressed in human adult astrocytes and not in HFA. However, in this study, we found Cx43 to be highly expressed at the mRNA level in HFA. Therefore, further studies are warranted to investigate the marker expression and functional capacity of human adult astrocytes. One of the main limiting factors for conducting studies of this type is the lack of protocols for efficiently sorting astrocytes from adult tissue. In fact, one of the only techniques effective in isolating astrocytes is immunopanning, used by the late Dr. Barres' lab (Cahoy et al., 2008; Sloan & Barres, 2014). However, one of the limitations of this technique is that other teams have not been able to use it successfully. Another limitation is the number of astrocytes that are extracted using this method are low (~500,000 cells), which is not representative of the number of astrocytes within a given tissue that has 1 billion cells, since astrocytes are the most abundant cell type in the human brain tissue. As a result, the first step in conducting studies discriminating between adult and fetal astrocytes is to develop techniques to efficiently obtain astrocytes from human adult tissue.

Further, at the NPC stage of development, we can explore other avenues of producing NPCs from stem cells. For example, we can use 3D models of development, including embryoid bodies and neurospheres, and comparing them to the current model of development, which is an entirely 2D model. We can then evaluate these NPCs for astrocytic, neuronal and NPC marker expression, as well as their capacity to differentiate into oligodendrocytes, neurons and astrocytes, in order to evaluate their quality. Perhaps developing NPCs from a 3D model, which

may emulate the *in vivo* process better, can result in better NPCs. Further, developing NPCs using the current 2D method may result in driving the development towards an astrocytic fate from the beginning, which may explain the high mRNA levels of astrocytic markers.

The next aim of this study was to compare stem-cell derived astrocytes, using protocol 2, from ALS patients to their age- and sex-matched controls. As shown in Figure 13, ALS astrocytes had lower mRNA levels of NESTIN and EAAT2, and higher mRNA levels of GS, TGF-B1 and CX43. These changes corroborate with changes observed in ALS animal models and post-mortem tissue (Almad et al., 2017; Bos et al., 2006; Ghoddoussi et al., 2010; Liu & Martin, 2006; Wallis, Zagami, Beart, & O'Shea, 2012a).

Several lines of evidence have shown that ALS is not a cell-autonomous disease, and astrocytes are one of the cell types contributing to the disease development and progression (Boillée, Vande Velde, & Cleveland, 2006; Nagai et al., 2007; Pramatarova et al., 2001). One of the proposed mechanisms underlying development of ALS is glutamate excitotoxicity (Corona, Tovar-y-Romo, & Tapia, 2007). Glutamate excitotoxicity may result from abnormally high levels of glutamate in the synapse, partially due to lower rate of glutamate reuptake by the neuron and/or astrocytes. Specifically in ALS, lower EAAT2 levels have been observed previously in both animal models and post mortem human tissue (Lin et al., 2013), and we observed lower levels of EAAT2 mRNA in stem-cell derived astrocytes in this study as well. EAAT2 is a glutamate transporter, responsible for the majority of glutamate uptake by astrocytes in some areas of the CNS. Lower levels of EAAT2 may result in less glutamate uptake by the astrocytes, therefore leaving more excess glutamate in the synapse and contributing to glutamate excitotoxicity. In addition to lower levels of EAAT2, stem-cell derived astrocytes from ALS patients also had higher levels of glutamate synthetase, which has been shown before in ALS patients (Bos et al.,

2006). Glutamate synthetase is an enzyme in astrocytes that converts the glutamate taken up from the synapse to glutamine, and the glutamine can then be sent back to the pre-synaptic neuron to be recycled and converted to glutamate (Suárez et al., 2002). One study found that higher levels of GS resulted in higher levels of glutamate in the synapse, and inhibiting GS reduced the levels of synaptic glutamate in SOD1G93A mice (Ghoddoussi et al., 2010). Moreover, inhibiting GS resulted in 8% increase in lifespan of these mice. Therefore, a reduction in EAAT2 and increase in GS may partially contribute to disease development and progression in ALS, and were observed in astrocytes derived from stem cells of ALS patients with SOD1 mutation.

Another astrocyte-specific protein associated with ALS is Cx43. Cx43 is one of the main gap junction proteins in astrocytes, and its expression has been shown to higher in ALS astrocytes in animal models, as well as in stem-cell derived astrocytes from ALS patients with SOD1 mutation (Almad et al., 2017). Indeed, we made the same observation in stem-cell derived astrocytes from ALS patients with SOD1 mutation. Interestingly, high levels of Cx43 can contribute to the toxicity induced in motor neurons by astrocytes in ALS. In fact, when Cx43 was inhibited in astrocytes with mutated SOD1, motor neurons survival doubled (Almad et al., 2017).

Another change we observed was lower levels of NESTIN mRNA in ALS astrocytes compared to controls. In SOD1G93A mice, lower levels of NESTIN was also observed in the neural stem cells of the subventricular zone, post-symptom onset (Liu & Martin, 2006). However, this change was not evident before the onset of symptoms. As discussed before, there is a heterogeneous population cells in the cultures derived from stem cells, including NPCs. In this study, we observed changes in NPCs in the culture as well, suggesting that even at the NPC stage, these cells may recapitulate the disease and be valuable for studying ALS, due to the fact

that these changes in NESTIN protein levels have been observed before in SOD1 ALS (Liu & Martin, 2006). Since we also observe these changes, it may suggest that these cultures, although not fully mature, may be relatively similar to adult cells.

Release of toxic factors by astrocytes has been proposed as a potential mechanism contributing to disease development and progression in ALS. One toxic factor proposed to be partially responsible for the astrocytic toxicity towards motor neurons is TGFB1, which was released at high levels from SOD1G93A mouse astrocytes (Tripathi et al., 2017). In fact, when TGFB1 levels were reduced, motor neuron death was reduced. In this study, we also found modest, but significant increase in the mRNA levels of TGFB1. Another toxic factor found to be released at high levels from ALS astrocytes is S100B. S100B has been shown to be higher in rodent astrocytes from ALS models with SOD1 mutation (Serrano et al., 2017), but we did not observe these changes in stem-cell derived astrocytes. Other changes observed previously in ALS, associated with SOD1, that we did not observe in this study were changes in AQP4, Kir4.1 and ALDH1L1 levels (Bataveljic et al., 2012; Kelley et al., 2018). This may be due to the lack of maturity in these astrocytes, or due to the fact that we only assessed one biological replicate of each cell line. Therefore, to confirm no change in the mRNA of these proteins, we need to repeat these experiments in more biological replicates. Beyond the variation in biological replicates, there is also differences between human and rodent astrocytes. Since most of the changes have been observed in rodent models, it may be true that there are other mechanisms involved, incorporating changes in other markers. This may be especially true since most effective treatments in ALS mouse models did not translate to humans (Benatar, 2007).

Now that we have shown that at the mRNA level, these stem-cell derived astrocytes show some of the changes previously observed in other models of ALS with SOD1 mutation, we can also

evaluate the protein levels of these markers. In addition to the markers explored, GFAP, a marker associated with increased activation in astrocytes (Wallis, Zagami, Beart, & O'Shea, 2012b), needs to be measured at the mRNA and protein level. In order to assess morphological changes, astrocytes from ALS patients should be stained with GFAP (activation marker) and S100B. Further, functional changes in these astrocytes also need to be evaluated. For example, since we have shown lower levels of EAAT2 mRNA, we also need to investigate whether glutamate uptake is also less efficient by these stem-cell derived astrocytes from ALS patients. In addition, investigating the toxicity of astrocytes to neurons is also warranted. For these experiments, we could co-plate ALS astrocytes with control neurons to evaluate the rate of neuronal cell death. Beyond investigating astrocytes with ALS with SOD1 mutations, it will also be interesting to investigate astrocytes from ALS patients with other mutations, such as FUS, C9orf72 or TDP43 mutations.

Further, in this study, control astrocytes came from age- and sex-matched healthy subjects. However, the gold standard for control cell lines is isogenic cell lines, in which the mutation is corrected, and the cell lines are otherwise the same. Therefore, another future direction for this study will be to create isogenic control cell lines for each of the patient cell lines, and repeat the experiments to ensure that all phenotypes remain and potentially discover new phenotypes.

Conclusion

In this study, we attempted to evaluate astrocytes derived from three different protocols for astrocytic maturity. We found that astrocytes from all protocols expressed key astrocytic markers, such as GFAP, S100B, EAAT1, EAAT2, AQP4, Kir4.1, ALDH1L1 and GAT3. Although these astrocytes expressed astrocytic markers, they may not have been mature. Therefore, we can conclude that all protocols result in immature astrocytes. However, when

assessing morphology, we can see that astrocytes derived from protocols 1 and 2 were more mature because they were bigger and had more projections, which are both characteristics of more mature astrocytes.

Further, we used protocol 2 to derived astrocytes from 3 ALS patients with SOD1 mutation and their age- and sex-matched controls. Interestingly, we found that at the mRNA level, these astrocytes expressed changes previously observed in other studies investigating ALS pathogenesis in animal models and post-mortem tissue. Specifically, we found lower levels of NESTIN and EAAT2, and higher levels of Cx43, GS and TGF-B1. Therefore, although not fully mature, these astrocytes may recapitulate the human disease appropriately, therefore offering a model system to study ALS in.

References

- Alexianu, M. E., Kozovska, M., & Appel, S. H. (2001). Immune reactivity in a mouse model of familial ALS correlates with disease progression. *Neurology*, *57*(7), 1282–1289.
<https://doi.org/10.1212/WNL.57.7.1282>
- Almad, A. A., Doreswamy, A., Gross, S. K., Richard, J., Haughey, N., & Maragakis, N. J. (2017). Connexin 43 in astrocytes contributes to motor neuron toxicity in amyotrophic lateral sclerosis. *Glia*, *64*(7), 1154–1169. <https://doi.org/10.1002/glia.22989>. Connexin
- Anthony, T. E., & Heintz, N. (2007). The Folate Metabolic Enzyme ALDH1L1 Is Restricted to the Midline of the Early CNS , Suggesting a Role in Human Neural Tube Defects. *The Journal of Comparative Neurology*, *500*, 368–383. <https://doi.org/10.1002/cne>
- Bar-peled, O., Ben-hur, H., Biegon, A., Groner, Y., Dewhurst, S., Furuta, A., & Rothstein, J. D. (1997). Distribution of Glutamate Transporter Subtypes During Human Brain Development. *Journal of Neurochemistry*, *69*(6), 2571–2580.
- Barnabé-Heider, F., Wasylnka, J. A., Fernandes, K. J. L., Porsche, C., Sendtner, M., Kaplan, D. R., & Miller, F. D. (2005). Evidence that embryonic neurons regulate the onset of cortical gliogenesis via cardiotrophin-1. *Neuron*, *48*(2), 253–265.
<https://doi.org/10.1016/j.neuron.2005.08.037>
- Bataveljic, D., Nikolic, L., Milosevic, M., Todorovic, N., & Andjus, P. (2012). Changes in the Astrocytic Aquaporin-4 and Inwardly Rectifying Potassium Channel Expression in the Brain of the Amyotrophic Lateral Sclerosis SOD1 G93A Rat Model. *Glia*, *60*, 1991–2003.
<https://doi.org/10.1002/glia.22414>

- Bell, S., Peng, H., Crapper, L., Kolobova, I., Maussion, G., Vasuta, C., ... Ernst, C. (2016). A rapid pipeline to model rare neurodevelopmental disorders with simultaneous CRISPR/Cas9 gene editing. *Stem Cell Translational Medicine*, 668–672.
- Benatar, M. (2007). Lost in translation : Treatment trials in the SOD1 mouse and in human ALS, 26, 1–13. <https://doi.org/10.1016/j.nbd.2006.12.015>
- Boillée, S., Vande Velde, C., & Cleveland, D. W. (2006). ALS: A Disease of Motor Neurons and Their Nonneuronal Neighbors. *Neuron*, 52(1), 39–59.
<https://doi.org/10.1016/j.neuron.2006.09.018>
- Boillée, S., Yamanaka, K., Lobsiger, C. S., Copeland, N. G., Jenkins, N. a, Kassiotis, G., ... Cleveland, D. W. (2006). Onset and progression in inherited ALS determined by motor neurons and microglia. *Science (New York, N.Y.)*, 312(5778), 1389–1392.
<https://doi.org/10.1126/science.1123511>
- Bos, I. W. M., Hoogland, G., Meine Jansen, C. F., Van Willigen, G., Spierenburg, H. A., Van Den Berg, L. H., & De Graan, P. N. E. (2006). Increased glutamine synthetase but normal EAAT2 expression in platelets of ALS patients. *Neurochemistry International*, 48(4), 306–311. <https://doi.org/10.1016/j.neuint.2005.09.009>
- Bunton-stasyshyn, R. K. A., Saccon, R. A., Fratta, P., & Fisher, E. M. C. (2015). SOD1 Function and Its Implications for Amyotrophic Lateral Sclerosis Pathology : New and Renascent Themes. *The Neuroscientist*, 21(5), 519–529. <https://doi.org/10.1177/1073858414561795>
- Cahoy, J. D., Emery, B., Kaushal, A., Foo, L. C., Zamanian, J. L., Christopherson, K. S., ... Barres, B. A. (2008). A Transcriptome Database for Astrocytes, Neurons, and Oligodendrocytes: A New Resource for Understanding Brain Development and Function.

The Journal of Neuroscience, 28(1), 264–278. <https://doi.org/10.1523/JNEUROSCI.4178-07.2008>

Chandrasekaran, A., Avci, H. X., Leist, M., Kobolák, J., & Dinnyés, A. (2016). Astrocyte Differentiation of Human Pluripotent Stem Cells: New Tools for Neurological Disorder Research. *Frontiers in Cellular Neuroscience*, 10(September), 215. <https://doi.org/10.3389/fncel.2016.00215>

Charrigre-bertrand, C., Garner, C., Tardy, M., & Nunez, J. (1991). Expression of Various Microtubule-Associated Protein 2 Forms in the Developing Mouse Brain and in Cultured Neurons and Astrocytes. *Journal of Neurochemistry*, 56(2), 385–391.

Christopherson, K. S., Ullian, E. M., Stokes, C. C. A., Mullowney, C. E., Hell, J. W., Agah, A., ... Barres, B. A. (2005). Thrombospondins are astrocyte-secreted proteins that promote CNS synaptogenesis. *Cell*, 120(3), 421–433. <https://doi.org/10.1016/j.cell.2004.12.020>

Clement, A. M., Nguyen, M. D., Roberts, E. A., Garcia, M. L., Boillée, S., Rule, M., ... Cleveland, D. W. (2003). Wild-type nonneuronal cells extend survival of SOD1 mutant motor neurons in ALS mice. *Science (New York, N.Y.)*, 302(5642), 113–7. <https://doi.org/10.1126/science.1086071>

Corona, J. C., Tovar-y-Romo, L. B., & Tapia, R. (2007). Glutamate excitotoxicity and therapeutic targets for amyotrophic lateral sclerosis. *Expert Opinion on Therapeutic Targets*, 11(11), 1415–1428. <https://doi.org/10.1517/14728222.11.11.1415>

Dadon-Nachum, M., Melamed, E., & Offen, D. (2011). The “dying-back” phenomenon of motor neurons in ALS. *Journal of Molecular Neuroscience*, 43(3), 470–477. <https://doi.org/10.1007/s12031-010-9467-1>

- Dermietzel, R., Traub, O., Hwang, T. K., Beyer, E., Bennet, M. V. L., Spray, D. C., & Willecke, K. (1989). Differential expression of three gap junction proteins in developing and mature brain tissues. *Proceedings of the National Academy of Sciences*, *86*(December), 10148–10152.
- Díaz-amarilla, P., Olivera-bravo, S., Trias, E., Cragolini, A., Martínez-palma, L., Cassina, P., ... Barbeito, L. (2011). Phenotypically aberrant astrocytes that promote motoneuron damage in a model of inherited amyotrophic lateral sclerosis. *PNAS*, *108*(44), 18126–31. <https://doi.org/10.1073/pnas.1110689108>
- Freeman, M. R. (2010). Specification and morphogenesis of astrocytes. *Science*, *330*(6005), 774–778. <https://doi.org/10.1126/science.1190928>.Specification
- Geevasinga, N., Menon, P., Ng, K., Van Den Bos, M., Byth, K., Kiernan, M. C., & Vucic, S. (2016). Riluzole exerts transient modulating effects on cortical and axonal hyperexcitability in ALS. *Amyotrophic Lateral Sclerosis and Frontotemporal Degeneration*, *17*(7–8), 580–588. <https://doi.org/10.1080/21678421.2016.1188961>
- Ghoddoussi, F., Galloway, M. P., Jambekar, A., Bame, M., Needleman, R., & Brusilow, W. S. A. (2010). Methionine sulfoximine, an inhibitor of glutamine synthetase, lowers brain glutamine and glutamate in a mouse model of ALS. *Journal of the Neurological Sciences*, *290*(1–2), 41–47. <https://doi.org/10.1016/j.jns.2009.11.013>
- Goetz, C. G. (2000). Amyotrophic lateral sclerosis: Early contributions of Jean-Martin Charcot. *Muscle and Nerve*, *23*(3), 336–343. [https://doi.org/10.1002/\(SICI\)1097-4598\(200003\)23:3<336::AID-MUS4>3.0.CO;2-L](https://doi.org/10.1002/(SICI)1097-4598(200003)23:3<336::AID-MUS4>3.0.CO;2-L)
- Gorshkov, K., Aguisanda, F., Thorne, N., & Zheng, W. (2018). Astrocytes as targets for drug

discovery. *Drug Discovery Today*, 00(00). <https://doi.org/10.1016/j.drudis.2018.01.011>

Haidet-phillips, A. M., Hester, M. E., Miranda, C. J., Meyer, K., Braun, L., Frakes, A., ...

Kaspar, B. K. (2012). Astrocytes from familial and sporadic ALS patients are toxic to motor neurons. *Nature Biotechnology*, 29(9), 824–828.

<https://doi.org/10.1038/nbt.1957.Astrocytes>

Jack, C. S., Arbour, N., Manusow, J., Montgrain, V., Blain, M., Mccrea, E., ... Antel, J. P.

(2005). TLR Signaling Tailors Innate Immune Responses in Human Microglia and Astrocytes. *Journal of Immunology*, 175, 4320–4330.

<https://doi.org/10.4049/jimmunol.175.7.4320>

Kelley, K. W., Ben Haim, L., Schirmer, L., Tyzack, G. E., Tolman, M., Miller, J. G., ...

Rowitch, D. H. (2018). Kir4.1-Dependent Astrocyte-Fast Motor Neuron Interactions Are Required for Peak Strength. *Neuron*, 98(2), 306–319.e7.

<https://doi.org/10.1016/j.neuron.2018.03.010>

Kimelberg, H. K., & Nedergaard, M. (2010). Functions of Astrocytes and their Potential As

Therapeutic Targets. *Neurotherapeutics*, 7(4), 338–353.

<https://doi.org/10.1016/j.nurt.2010.07.006>

Kolahdouzan, M., & Hamadeh, M. (2017). The neuroprotective effects of caffeine in

neurodegenerative diseases. *CNS Neurosci Ther*, 23(0), 272–290.

<https://doi.org/10.1111/cns.12684>

Krencik, R., Weick, J. P., Liu, Y., Zhang, Z., & Zhang, S.-C. (2011). Specification of

transplantable astroglial subtypes from human pluripotent stem cells. *Nature Biotechnology*, 29(6), 528–534. <https://doi.org/10.1038/nbt.1877.Specification>

- Krencik, R., & Zhang, S.-C. (2011). Directed Differentiation of Functional Astroglial Subtypes from Human Pluripotent Stem Cells. *Nat Protoc.*, 6(11), 1710–1717.
<https://doi.org/10.1038/nprot.2011.405>.Directed
- Kriz, J., Nguyen, M. D., & Julien, J. P. (2002). Minocycline slows disease progression in a mouse model of amyotrophic lateral sclerosis. *Neurobiology of Disease*, 10(3), 268–278.
<https://doi.org/10.1006/nbdi.2002.0487>
- Lasiene, J., & Yamanaka, K. (2011). Glial cells in amyotrophic lateral sclerosis. *Neurology Research International*, 2011. <https://doi.org/10.1155/2011/718987>
- Lin, C.-L. G., King, Q., Cuny, G. D., & Glicksman, M. A. (2013). Glutamate transporter EAAT2: a new target for the treatment of neurodegenerative diseases. *Future Med Chem*, 4(13), 1689–1700. <https://doi.org/10.4155/fmc.12.122>.Glutamate
- Liu, Z., & Martin, L. J. (2006). The adult neural stem and progenitor cell niche is altered in amyotrophic lateral sclerosis mouse brain. *The Journal of Comparative Neurology*, 497, 468–488. <https://doi.org/10.1002/cne>
- Madill, M., Mcdonagh, K., Ma, J., Vajda, A., Mcloughlin, P., & Brien, T. O. (2017). Amyotrophic lateral sclerosis patient iPSC- derived astrocytes impair autophagy via non-cell autonomous mechanisms. *Molecular Brain*, 10(22), 1–12.
<https://doi.org/10.1186/s13041-017-0300-4>
- Maragakis, N. J., & Rothstein, J. D. (2006). Mechanisms of Disease: astrocytes in neurodegenerative disease. *Nature Clinical Practice Neurology*, 2(12), 679–689.
<https://doi.org/10.1038/ncpneuro0355>

- Marchetto, M. C. N., Muotri, A. R., Mu, Y., Smith, A. M., Cezar, G. G., & Gage, F. H. (2008). Article Non-Cell-Autonomous Effect of Human SOD1 G37R Astrocytes on Motor Neurons Derived from Human Embryonic Stem Cells. *Stem Cell*, 3(6), 649–657. <https://doi.org/10.1016/j.stem.2008.10.001>
- Meyer, K., Ferraiuolo, L., Miranda, C. J., Likhite, S., Mcelroy, S., & Rensch, S. (2014). Direct conversion of patient fibroblasts demonstrates non-cell autonomous toxicity of astrocytes to motor neurons in familial and sporadic ALS. *Proceedings of the National Academy of Sciences*, 111(2), 829–832. <https://doi.org/10.1073/pnas.1314085111>
- Mohammad, M. H., Al-Shammari, A. M., Al-Juboory, A. A., & Yaseen, N. Y. (2016). Characterization of neural stemness status through the neurogenesis process for bone marrow mesenchymal stem cells. *Stem Cell and Cloning: Advances and Applications*, 9, 1–15.
- Molofsky, A. V., & Deneen, B. (2015). Astrocyte development: A Guide for the Perplexed. *Glia*, 63(8), 1320–1329. <https://doi.org/10.1002/glia.22836>
- Nadarajah, B., Jones, A. M., Evans, W. H., & Parnavelas, J. G. (1997). Differential Expression of Connexins during Neocortical Development and Neuronal Circuit Formation. *The Journal of Neuroscience*, 17(9), 3096–3111.
- Nagai, M., Re, D. B., Nagata, T., Chalazonitis, A., Jessel, T. M., Wichterle, H., & Przedborski, S. (2007). Astrocytes expressing ALS-linked mutated SOD1 release factors selectively toxic to motor neurons. *Nature Neuroscience*, 10(5), 615–622. <https://doi.org/10.1038/nn1876>.Astrocytes
- Noctor, S. C., Martínez-cerdeño, V., Ivic, L., & Kriegstein, A. R. (2004). Cortical neurons arise

- in symmetric and asymmetric division zones and migrate through specific phases. *Nature Neuroscience*, 7(2), 136–144. <https://doi.org/10.1038/nn1172>
- Okada, M., Yamashita, S., Ueyama, H., Ishizaki, M., Maeda, Y., & Ando, Y. (2018). Long-term effects of edaravone on survival of patients with amyotrophic lateral sclerosis. *ENeurologicalSci*, 11(May), 11–14. <https://doi.org/10.1016/j.ensci.2018.05.001>
- Papadeas, S. T., Kraig, S. E., O'Banion, C., Lepore, A. C., & Maragakis, N. J. (2011). Astrocytes carrying the superoxide dismutase 1 (SOD1G93A) mutation induce wild-type motor neuron degeneration in vivo. *Proceedings of the National Academy of Sciences*, 108(43), 17803–17808. <https://doi.org/10.1073/pnas.1103141108>
- Paşca, A. M., Sloan, S. A., Clarke, L. E., Tian, Y., & Christopher, D. (2015). Functional cortical neurons and astrocytes from human pluripotent stem cells in 3D culture. *Nature Methods*, 12(7), 671–678. <https://doi.org/10.1038/nmeth.3415>. Functional
- Pasinelli, P., & Brown, R. H. (2006). Molecular biology of amyotrophic lateral sclerosis: insights from genetics. *Nature Reviews. Neuroscience*, 7(9), 710–723. <https://doi.org/10.1038/nrn1971>
- Pramatarova, A., Laganière, J., Roussel, J., Brisebois, K., & Rouleau, G. A. (2001). Neuron-specific expression of mutant superoxide dismutase 1 in transgenic mice does not lead to motor impairment. *The Journal of Neuroscience : The Official Journal of the Society for Neuroscience*, 21(10), 3369–74. <https://doi.org/21/10/3369> [pii]
- Qian, K., Huang, H., Peterson, A., Hu, B., Maragakis, N. J., Ming, G., ... Zhang, S.-C. (2017). Sporadic ALS astrocytes induce neuronal degeneration in vivo. *Stem Cell Reports*, 8(4), 843–855. <https://doi.org/10.1016/j.stemcr.2017.03.003>

- Raponi, E., Agenes, F., Delphin, C., Assard, N., Baudier, J., Legraverend, C., & Deloulme, J. C. (2007). S100B expression defines a state in which GFAP-expressing cells lose their neural stem cell potential and acquire a more mature developmental stage. *Glia*, *55*(2), 165–177. <https://doi.org/10.1002/glia.20445>
- Rojas, F., Cortes, N., Abarzua, S., Dyrda, A., & van Zundert, B. (2014). Astrocytes expressing mutant SOD1 and TDP43 trigger motoneuron death that is mediated via sodium channels and nitroxidative stress. *Frontiers in Cellular Neuroscience*, *8*(February), 24. <https://doi.org/10.3389/fncel.2014.00024>
- Rosen, D. R., Siddique, T., Patterson, D., Figlewicz, D. a, Sapp, P., Hentati, a, ... Deng, H. X. (1993). Mutations in Cu/Zn superoxide dismutase gene are associated with familial amyotrophic lateral sclerosis. *Nature*, *362*(6415), 59–62. <https://doi.org/10.1038/362059a0>
- Roybon, L., Lamas, N. J., Garcia, A. D., Yang, E. J., Sattler, R., Lewis, V. J., ... Henderson, C. E. (2013). Human stem cell-derived spinal cord astrocytes with defined mature or reactive phenotypes. *Cell Reports*, *4*(5), 1035–1048. <https://doi.org/10.1016/j.celrep.2013.06.021>.Human
- Sacson, R. A., Bunton-stasyshyn, R. K. A., Fisher, E. M. C., & Fratta, P. (2013). Is SOD1 loss of function involved in amyotrophic lateral sclerosis? *Brain : A Journal of Neurology*, *136*, 2342–2358. <https://doi.org/10.1093/brain/awt097>
- Santos, R., Vadodaria, K. C., Jaeger, B. N., Mei, A., Lefcochilos-fogelquist, S., Mendes, A. P. D., ... Gage, F. H. (2017). Differentiation of inflammation-responsive astrocytes from glial progenitors generated from human induced pluripotent stem cells. *Stem Cell Reports*, *8*(6), 1757–1769. <https://doi.org/10.1016/j.stemcr.2017.05.011>

- Schousboe, A., Bak, L. K., & Waagepetersen, H. S. (2013). Astrocytic control of biosynthesis and turnover of the neurotransmitters glutamate and GABA. *Frontiers in Endocrinology*, 4(AUG), 1–11. <https://doi.org/10.3389/fendo.2013.00102>
- Serio, A., Bilican, B., Barmada, S. J., Ando, D. M., Zhao, C., Siller, R., ... Chandran, S. (2013). Astrocyte pathology and the absence of non-cell autonomy in an induced pluripotent stem cell model of TDP-43 proteinopathy. *Proceedings of the National Academy of Sciences of the United States of America*, 110(12), 4697–702. <https://doi.org/10.1073/pnas.1300398110>
- Serrano, A., Donno, C., Giannetti, S., Perić, M., Andjus, P., D'Ambrosi, N., & Michetti, F. (2017). The Astrocytic S100B Protein with Its Receptor RAGE Is Aberrantly Expressed in SOD1G93A Models, and Its Inhibition Decreases the Expression of Proinflammatory Genes. *Mediators of Inflammation*, 2017. <https://doi.org/10.1155/2017/1626204>
- Shaltouki, A., Peng, J., Liu, Q., Rao, M. S., & Zeng, X. (2013). Efficient generation of astrocytes from human pluripotent stem cells in defined conditions. *Stem Cells*, 31, 941–952. <https://doi.org/10.1002/stem.1334>
- Shaw, P. J., & Eggett, C. J. (2000). Molecular factors underlying selective vulnerability of motor neurons to neurodegeneration in amyotrophic lateral sclerosis. *Journal of Neurology*, 247 Suppl, I17--I27. <https://doi.org/10.1007/BF03161151>
- Sloan, S. A., & Barres, B. A. (2014). Mechanisms of astrocyte development and their contributions to neurodevelopmental disorders. *Current Opinion in Neurobiology*, 27, 75–81. [https://doi.org/10.1016/S2215-0366\(16\)30284-X](https://doi.org/10.1016/S2215-0366(16)30284-X).Epidemiology
- Sloan, S. A., Darmanis, S., Huber, N., Khan, T. A., Birey, F., Caneda, C., ... Paşca, S. P. (2017). Human Astrocyte Maturation Captured in 3D Cerebral Cortical Spheroids Derived from

Pluripotent Stem Cells. *Neuron*, 95(4), 779–790.e6.

<https://doi.org/10.1016/j.neuron.2017.07.035>

Suárez, I., Bodega, G., & Fernández, B. (2002). Glutamine synthetase in brain: Effect of ammonia. *Neurochemistry International*, 41(2–3), 123–142. [https://doi.org/10.1016/S0197-0186\(02\)00033-5](https://doi.org/10.1016/S0197-0186(02)00033-5)

Takahashi, K., & Yamanaka, S. (2006). Induction of Pluripotent Stem Cells from Mouse Embryonic and Adult Fibroblast Cultures by Defined Factors. *Cell*, 126(4), 663–676. <https://doi.org/10.1016/j.cell.2006.07.024>

Taylor, J. P., Brown Jr, R. H., & Cleveland, D. W. (2016). Decoding ALS: from genes to mechanism. *Nature*, 539(7628), 197–206. <https://doi.org/10.1038/nature20413>.Decoding

TCW, J., Wang, M., Pimenova, A. A., Bowles, K. R., Hartley, B. J., Lacin, E., ... Brennand, K. J. (2017). An Efficient Platform for Astrocyte Differentiation from Human Induced Pluripotent Stem Cells. *Stem Cell Reports*, 9(2), 600–614. <https://doi.org/10.1016/j.stemcr.2017.06.018>

Thonhoff, J. R., Ojeda, L., & Wu, P. (2009). Stem cell-derived motor neurons: applications and challenges in amyotrophic lateral sclerosis. *Current Stem Cell Research & Therapy*, 4(3), 178–99. <https://doi.org/10.2174/157488809789057392>

Tripathi, P., Rodriguez-Muela, N., Klim, J. R., de Boer, A. S., Agrawal, S., Sandoe, J., ... Zhou, Q. (2017). Reactive Astrocytes Promote ALS-like Degeneration and Intracellular Protein Aggregation in Human Motor Neurons by Disrupting Autophagy through TGF- β 1. *Stem Cell Reports*, 9(2), 667–680. <https://doi.org/10.1016/j.stemcr.2017.06.008>

- Vargas, M. R., & Johnson, J. a. (2010). Astrogliosis in amyotrophic lateral sclerosis: role and therapeutic potential of astrocytes. *Neurotherapeutics : The Journal of the American Society for Experimental NeuroTherapeutics*, 7(4), 471–481.
<https://doi.org/10.1016/j.nurt.2010.05.012>
- Wallis, N., Lau, C. L., Farg, M. A., Atkin, J. D., Beart, P. M., & O’Shea, R. D. (2017). SOD1 Mutations Causing Familial Amyotrophic Lateral Sclerosis Induce Toxicity in Astrocytes: Evidence for Bystander Effects in a Continuum of Astrogliosis. *Neurochemical Research*, 0(0), 1–14. <https://doi.org/10.1007/s11064-017-2385-7>
- Wallis, N., Zagami, C. J., Beart, P. M., & O’Shea, R. D. (2012a). Combined excitotoxic-oxidative stress and the concept of non-cell autonomous pathology of ALS: Insights into motoneuron axonopathy and astrogliosis. *Neurochemistry International*, 61(4), 523–530.
<https://doi.org/10.1016/j.neuint.2012.02.026>
- Wallis, N., Zagami, C. J., Beart, P. M., & O’Shea, R. D. (2012b). Combined excitotoxic-oxidative stress and the concept of non-cell autonomous pathology of ALS: Insights into motoneuron axonopathy and astrogliosis. *Neurochemistry International*, 61(4), 523–530.
<https://doi.org/10.1016/j.neuint.2012.02.026>
- Watanabe-Matsumoto, S., Moriwaki, Y., Okuda, T., Ohara, S., Yamanaka, K., Abe, Y., ... Misawa, H. (2017). Dissociation of blood-brain barrier disruption and disease manifestation in an aquaporin-4-deficient mouse model of amyotrophic lateral sclerosis. *Neuroscience Research*, 4, 1–10. <https://doi.org/10.1016/j.neures.2017.11.001>
- Yamanaka, K., Boillee, S., Roberts, E. A., Garcia, M. L., McAlonis-Downes, M., Mikse, O. R., ... Goldstein, L. S. B. (2008). Mutant SOD1 in cell types other than motor neurons and

oligodendrocytes accelerates onset of disease in ALS mice. *Proceedings of the National Academy of Sciences*, *105*(21), 7594–7599. <https://doi.org/10.1073/pnas.0802556105>

Yamanaka, K., Chun, S. J., Boillee, S., Fujimori-tonou, N., Gutmann, D. H., Takahashi, R., ... Cleveland, D. W. (2008). Astrocytes as determinants of disease progression in inherited ALS. *Nature Neuroscience*, *11*(3), 251–253. <https://doi.org/10.1038/nn2047>.Astrocytes

Yamanaka, K., & Komine, O. (2017). The multi-dimensional roles of astrocytes in ALS. *Neuroscience Research*, *126*, 31–38. <https://doi.org/10.1016/j.neures.2017.09.011>

Zhang, Y., Sloan, S. A., Clarke, L. E., Caneda, C., Plaza, C. A., Blumenthal, P. D., ... Barres, B. A. (2016). Purification and characterization of progenitor and mature human astrocytes reveals transcriptional and functional differences with mouse. *Neuron*, *89*(1), 37–53. <https://doi.org/10.1016/j.neuron.2015.11.013>.Purification